EFFECT OF CONCENTRATION OF REACTANTS AND DEPOSITION TEMPERATURE ON THE OPTICAL PROPERTIES OF IRON-DOPED CADMIUM STANNATE THIN FILMS DEPOSITED ON GLASS SUBSTRATES BY SPRAY PYROLYSIS

BY

ONGWEN NICHOLAS OGADA

A THESIS SUBMITTED IN PARTIAL FULFILLMENT OF THE REQUIREMENTS FOR THE DEGREE OF MASTER OF SCIENCE IN PHYSICS

DEPARTMENT OF PHYSICS & MATERIALS SCIENCE

MASENO UNIVERSITY

DECLARATION

This thesis is my original work and has not been presented in any institution of higher learning that I know of, for the award of a degree certificate.

ONGWEN NICHOLAS OGADA

MSc/Sc/00038/015

Signature…… Date……

This thesis has been submitted for examination with our approval as the supervisors:

1. Prof. Andrew O. Oduor,
Department of Physics and Materials Science,
Maseno University,
P. O. Box 333-40105,
Maseno-Kenya.

Signature……..... Date……

2. Dr. Elijah O. Ayieta,
Department of Physics, University of Nairobi,
P.O. Box 30197-00100,
Nairobi-Kenya.

Signature…….. Date……

ACKNOWLEDGEMENT

My foremost sincere gratitude goes to the Almighty God for giving me this opportunity (life, health, mind, and strength) to come up with this work. He has guided me this far I have reached, providing me with knowledge.

I would also like to appreciate my supervisor, Professor Andrew O. Oduor for his endless support and helping hand whenever I needed assistance. He always worked tirelessly to ensure that this study was carried out successfully, by giving me directions and making corrections in the work, up to the final draft.

Special thanks go to Doctor Elijah O. Ayieta for acting as the co-supervisor for the study and also for providing me with experimental supervision. He was always with me whenever I needed any assistance.

Sincere gratitude goes to my loving wife, Celestine Achieng Ogada, who has been giving me constant encouragement, moral support, care and a conducive study environment in order to come up with this work. She was supportive throughout my studies.

I will not forget to appreciate the assistance that I received from Dr. Henry Otunga, Dr. George Omondi and Mr. Austin Mulama (a Ph.D. student) all from Maseno University for their guidance on how to analyze data and how to arrange the components of my research work, as well as reading my thesis drafts and guiding me on the corrections to make; the lab technicians of Maseno University, who gave me orientation and assistance on the use of lab apparatus and equipment. They gave me a strong foundation and confidence on the use of the lab equipment, especially spectrophotometer and how to label samples

Special thanks also go to the laboratory technician at the University of Nairobi, Mr. Boniface Muthoka. He gave me all the experimental experience that I needed in order to carry out the research. He showed me how to use all the equipment that I needed for the research (spray pyrolysis, spectrophotometer and surface profiler), how to label the slides and how to take measurements using the spectrophotometer and the surface profiler.

Many thanks also go to Mrs. Sheila Bisach, a Master's student in Physics, University of Nairobi. She gave me the experimental experience that I needed and showed me how to use some of the equipment. She also showed me how to use Origin Lab, a graphical analysis software that I later used to analyze the data that I collected from the experiments.

I would also like to appreciate Mr. Dinfa Domtau, a Ph.D. student at the University of Nairobi, who gave me insight on how to carry out the experiment. I am greatly indebted to him.

Lastly, I would like to thank the National Research Fund (NRF) for funding the research during the 2016-2017 financial year.

DEDICATION

The Almighty God

My loving wife, Celestine Achieng Ogada

ABSTRACT

Thin films (TFs) have numerous applications in the modern technological world, ranging from energy production in TF solar cells/ photovoltaic (PV) cells to liquid crystal displays (LCDs) in television screens and in smartphone touch screens as transparent conducting oxides (TCOs). The most commonly used TCO material is indium tin oxide (ITO). However, ITO has two main drawbacks. Firstly, indium is expensive and secondly, it is rare. These drawbacks call for relatively cheaper compounds like cadmium stannate (Cd_2SnO_4). The TFs of Cd_2SnO_4 have been researched on and proved to possess excellent optical properties (transmittance, absorption coefficient and band gap), which are superior to most of the conventional TCO materials, including cadmium telluride (CdTe), copper-indium-gallium-diselenide and the ITO. The study of optical properties of Cd_2SnO_4 doped with metals such as zinc and yttrium has been done. However, the study of optical properties of Cd_2SnO_4 doped with Fe has not been done. This research thus studied the optical properties of Cd_2SnO_4 doped with Fe, deposited on glass substrates at temperatures of 350 °C, 400 °C and 450 °C. The specific objectives of the study were to determine the effect of (i) concentration of reactants and (ii) deposition temperature on the optical properties of Cd_2SnO_4: Fe. The Cd_2SnO_4 was prepared by mixing solutions of cadmium acetate and tin II chloride, both dissolved in ethanol at ratios of 0.1:0.1M, 0.2:0.2M and 0.3:0.3M, forming a white precipitate. 3ml of 2M hydrochloric acid was then added to the precipitate, after which it dissolved to form the colourless solution of Cd_2SnO_4. The Cd_2SnO_4 solution was then mixed with iron III chloride (the dopant) dissolved in ethanol at 0-8% concentration by volume of Cd_2SnO_4 and then sprayed onto the preheated microscope glass substrates by spray pyrolysis. The optical reflectance and transmittance were measured using spectrophotometer in the ultraviolet-visible-near-infrared wavelength range of 300-1100 nm, from which the optical constants were determined. It was found out that an increase in the concentration of the reactants reduced transmittance and band gap, but increased absorption coefficient, extinction coefficient and refractive index, which was. An increase in the deposition temperature increased transmittance and band gap but decreased absorption coefficient, extinction coefficient and refractive index, which was attributed to increase in crystallinity of the TFs. Doping reduced transmittance and band gap, but increased refractive index, absorption coefficient and extinction coefficient, which was attributed to increase in the free charge carriers. At the upper end of the visible spectrum, the values of the optical constants obtained were: transmittance of up to 78.45%, absorption coefficient of 4.022-5.522 x 10^4 cm^{-1}, extinction coefficient of 0.188-0.258, refractive index of 1.77-2.12 and band gap of 3.5-3.9 eV. The results obtained in this study provide a good alternative antireflective material for use in: front panel of TF solar cells, smartphone touch screens and television LED screens, since the TFs have high transmittance of ~ 80%, a high absorption coefficient of x 10^4 cm^{-1} and a large band gap of up to 3.9 eV, which are the ideal properties of TCO materials.

TABLE OF CONTENTS

LIST OF ABBREVIATIONS AND ACRONYMS

AFM	Atomic Force Microscope
CB	Conduction Band
CIGS	Copper-Indium-Gallium-Diselenide
C-Si	Crystalline Silicon
DI	Deionized
IR	Infrared
ITO	Indium Tin Oxide
LCD	Liquid Crystal Display
PV	Photovoltaic
SPT	Spray Pyrolysis Technique
TCO	Transparent Conducting Oxide
TF	Thin Film
UV-V-NIR	Ultraviolet-Visible-Near Infrared
VB	Valence Band
VET	Vacuum Evaporation Technique
XRD	X-Ray Diffraction
XPS	X-Ray Photoelectron Spectroscope.

LIST OF SYMBOLS

A	Optical absorbance
c	Speed of light
E_g	Optical band gap energy
I_o	Intensity of incident light
I_T	Intensity of transmitted light
k	Extinction coefficient
M	Molar
n	Refractive index
R	Optical reflectance
S	Siemens/ Scattered portion of the incident radiation
T	Optical transmittance
α	Optical absorption coefficient

LIST OF CHEMICAL SYMBOLS AND FORMULAE

Ar	Argon gas
$Ar\text{-}O_2$	Argon-Oxygen gas mixture
C	Carbon
Cd	Cadmium
Cd_2SnO_4	Cadmium Stannate
CdTe	Cadmium Telluride
Cl_2	Chlorine
Fe	Iron
H_2	Hydrogen gas
HCl	Hydrochloric acid
HNO_3	Nitric (V) acid
N_2	Nitrogen gas
Sn	Tin
Te	Tellurium
Y	Yttrium
Zn	Zinc

LIST OF TABLES

LIST OF FIGURES

LIST OF PUBLICATIONS

1. Effect of concentration of reactants on the optical properties of iron-doped cadmium stannate thin films deposited by spray pyrolysis.

   American Journal of Materials Science (Scientific and Academic Publishing)

2. Effect of deposition temperature on the optical properties of iron-doped cadmium stannate thin films deposited by spray pyrolysis.

   International Journal of Scientific and Technical Research in Engineering

CHAPTER ONE
INTRODUCTION

1.1 Background of the study

Transparent conducting oxide (TCO) thin films (TFs) have extensively been used in a variety of electronic and optoelectronic applications because of their high transmission in the visible region, high infrared reflection and low direct current resistivity. The great mass market for panel flat display is the main reason for TCO TFs research. The TCO film in practical applications nowadays is the tin-doped indium oxide, also known as indium tin oxide (ITO). However, ITO has two main drawbacks: Firstly, it is rare and secondly, it is expensive (Mazzeo et al, 2013). The above drawbacks of ITO call for cheaper and readily available materials for TCOs.

Recently, cadmium stannate (Cd_2SnO_4) has emerged as an excellent alternative candidate TCO material to the ITO due to its low cost as well as being abundant. Moreover, Cd_2SnO_4 is nontoxic and also has comparable optical properties to ITO, with a transmittance of up to 99%, a reflectance of as low as 1% and a band gap of 3.3 eV and above, making it be transparent over a large wavelength range (Krishna et al, 2010). Because Cd_2SnO_4 possesses desirable optical properties, its TFs have found a wide range of applications in transparent electrodes such as photovoltaic (PV) cells, liquid crystal displays (LCDs), window films and smartphone touch screens (Meysing et al, 2013) (Wu et al, 1997).

Most researches have focused on the improvement of electrical and optical properties of Cd_2SnO_4 TFs by optimizing conditions such as deposition temperature, annealing, addition of a second layer as well as doping it with non-metals like argon (Ar), nitrogen and chlorine (Cl_2); where the properties (electrical, electronic, optical and structural) have been found to improve. High deposition temperature has been found to favour the growth of bigger crystallites and the out-diffusion of oxygen to increase the number of oxygen vacancies. Consequently, the high-temperature condition increases the carrier mobility and carrier concentration of Cd_2SnO_4 TFs (Cristaldi et al, 2012).

Doping Cd_2SnO_4 with metals such as zinc (Zn) (Patil et al, 2012) and yttrium (Y) (Cristaldi et al, 2012) has also been done, although the studies did not consider the optical properties of the deposited TFs, but rather the structural, electrical and electronic. This study thus doped the TFs of Cd_2SnO_4 with a metal (iron) and then studied its optical properties within the wavelength range of 300-1100 nm.

Spray pyrolysis technique (SPT) was chosen as the method of deposition in this study because, compared to the other methods like sol-gel and vacuum evaporation technique (VET), it: is relatively cost-effective; does not require a vacuum, which may be difficult to maintain due to pump leakages; and does not require high-quality substrates (Gauckler, 2005).

1.2 Statement of the problem

ITO is the most common and widely known TCO material used in the fabrication of the window layers of TF PV solar cells, LCD screens of televisions and smartphone touchscreens. However, ITO has two existing drawbacks: scarcity and high cost of indium. These drawbacks limit the commercial deployment of the ITO. To produce low-cost and readily available TCO materials that can be used in the above-mentioned applications of ITO, explorative research is on-going to identify alternative TCO materials. TFs of Cd_2SnO_4 are potential candidates for use as TCO due to its improved optical properties (transmittance, absorption coefficient and band gap).

1.3 Objectives of the study

2.3.1. Main objective

The main objective was to study the optical properties: transmittance, absorption coefficient, extinction coefficient, refractive index and band gap of TFs of Cd_2SnO_4 doped with Fe at 0%, 2%, 4% and 8% doping concentrations and deposited on glass substrates by spray pyrolysis at temperatures of 350 °C, 400 °C and 450 °.

2.3.2. Specific objectives

The specific objectives of the study were:

i) To investigate the effect of concentration of reactants (cadmium, tin and iron) on the optical properties of iron-doped cadmium stannate thin films.

ii) To investigate the effect of deposition temperature on the optical properties of iron-doped cadmium stannate thin films.

1.4 Justification of the study

The main sources of electrical energy in Kenya are fossil fuel, hydroelectric power and geothermal, with fossil fuel accounting for 13%, hydroelectric power accounting for 30% while geothermal accounts for 47% (Kuo, 2017). Fossil fuel emits pollutant gases such as carbon oxides (carbon II oxide and carbon IV oxide) and sulphur oxides (sulphur IV oxide and sulphur VI oxide) into the atmosphere, causing environmental pollution, climate change and global warming. Kenya emits 0.03% of the global carbon IV oxide poisoning (Cole, 2013). Currently, Kenya is becoming a world leader in the number of solar power systems installed per capita. More Kenyans are turning to solar power rather than connections to the country's electricity grid. This is due to the relatively high connectivity cost of the grid and the abundance of solar power options in Kenya (Definitive solar, 2018). The solar cells must not only be less expensive, but also readily available.

The most dominant solar cell layer material is ITO. However, the two drawbacks of ITO (scarcity and high cost) call for research on alternative TCO materials that are not only cheaper, but also readily available. Due to the high demand for solar energy, other materials are being investigated. The elements in Cd_2SnO_4 are relatively cheaper and also readily available. The study of optical properties of iron-doped TFs of Cd_2SnO_4 is good for the formation of a window layer of TF solar cells and also for LCDs in televisions and smartphone touchscreens.

1.5 Significance of the study

The results of this study can find good use in coating screens of optoelectronic devices like smartphone touch screens and LCD screens in flat-screen televisions since the TF makes the glass antireflective, thus improving visibility. They can also be used in the front panels of TF solar cells that will allow more light energy to pass through the window and excite more electrons, enabling them to jump from the valence band (VB) to the conduction band (CB) in order to conduct electricity, thus improving the efficiency of the solar cells. Another potential use of the TFs from this study is in the window films that can be used as window panes to regulate the amount of heat entering the room by blocking the infrared (IR) during summer and allowing the IR to pass through and warm the rooms during winter.

1.6 Assumptions

The temperature of the heating plate dropped by about 7 °C when the spraying was started. Thus, the deposition temperatures were assumed to be the ones that were attained before spraying was started.

CHAPTER TWO
LITERATURE REVIEW

2.1. Introduction

In this chapter, an overview of desirable TCO materials for various applications is given. A review of the previous work that has been done on Cd_2SnO_4 is also given and the gaps in knowledge pointed out. The chapter also looks at the methods that have been applied in depositing TFs of Cd_2SnO_4 and the nature of the precursors that have been used. A review of TF optics is also given, where the equations for calculating the optical constants are given and explained. The chapter closes with a discussion on applications of TFs, including TF PV cells, LCDs and window films.

2.2. Thin film properties

2.2.1. Transmittance, reflectance and absorbance

Optical devices require transparent coating materials with varied degrees of light absorbance (A), reflectance (R) and transmittance (T). For example, a solar cell requires coating materials with high absorbance and transmittance, but low reflectance (antireflective) (Rauschenbach, 1980), (fig 2.1), while in an LCD screen, the matte coating (matte coating is a coating that is not smooth so as to enhance diffusion of ambient light) is included as an outer polarizing layer, which has been coarsened by mechanical or chemical processes (Baker, 2012). The matte finish achieves a coating which is not smooth and can diffuse ambient light rather than reflect it. Typically, the above applications use electrode materials that have greater than 80% transmittance of incident light and absorbance of less than 10% (Andreas, 2012).

The optical properties of TCOs are determined by refractive index, extinction coefficient, bandgap and geometry. An increase in reflectance/ absorbance increases refractive index, but decreases the transmittance, which is not desirable for TCO materials (Rakesh et al, 2018).

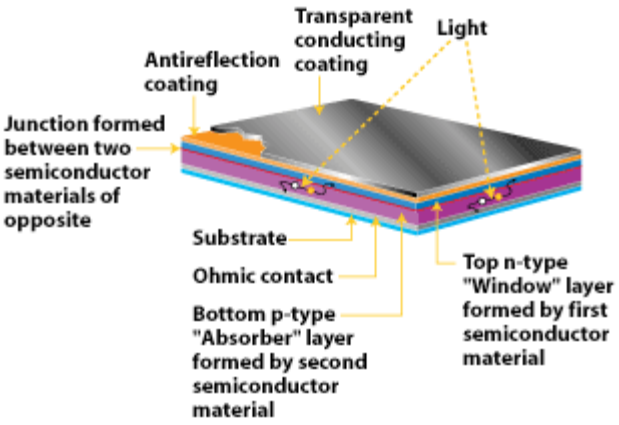

Figure 2.1: A typical thin-film silicon-based solar cell with a transparent conducting coating (https://en.m.wikipedia.org>wiki>transparent_conducting_film)

2.2.2. Absorption coefficient

Absorption coefficient describes the amount of light absorbed by a material medium per unit thickness of the material. The more the absorbance, the higher the absorption coefficient. Typical TCOs have an absorption coefficient of greater than $x10^4$ cm^{-1} in the UV-V-NIR wavelength (Coutts et al, 2000).

2.2.3. Extinction coefficient

Extinction coefficient is the imaginary part of the refractive index. The extinction coefficient of TCOs in the visible wavelength range is zero due to their large band gaps. In the UV wavelength range however, TCOs are usually opaque and extinction coefficient is non-zero because of the band-to-band absorption (a UV photon can excite an electron from the VB to the CB). TCOs are also opaque in the NIR and IR range because of free carrier absorption (an IR photon can excite an electron from near the bottom of the CB to a higher level within the CB) (Maity and Chattopadhyay, 2006).

.

In the NIR and IR regions, the extinction coefficient is non-zero and reaches its maximum value in the IR regime, similar to the behaviour of the extinction coefficient for metals. At the wavelength of 588 nm, ITO, the most common TCO has an extinction coefficient of 0.003 cm. TCOs should have extinction coefficients in the order of x 10^{-3} cm in order to achieve high transparency in the visible spectrum (Coutts et al, 2000).

2.2.4. Refractive index

Refractive index is a dimensionless quantity that describes how fast light propagates through a material medium. Refractive indices are usually measured at the wavelength of 588 nm. The optical properties of TCOs (transmittance, reflectance and absorbance) are determined by among other properties, the refractive index. Most TCOs have refractive indices in the range of 1.8-2.8. For instance, the refractive index of ITO, the most commonly used TCO at the 588 nm wavelength is 1.837. As refractive index increases in the visible spectral region, transmittance decreases, a property which is not desirable for TCOs, since the TCOs which should have as high transmittance as possible (Rakesh et al, 2018).

2.2.5. Band gap

TCOs possess wide band gaps whose energy values are greater than those of the visible light. As such, photon energies below the band gap value are not absorbed by the material and the visible light passes through, while those with energy larger than the band gap are absorbed. As a result, TCOs for use in TF solar cells should have a band gap of greater than 3.2 eV (Minami, 2005). ITO, the most common TCO material in TF solar cells has a large band gap of 3.5-4.3 eV (Du et al, 2014). Because of the large band gap, ITO is transparent in the visible portion of the spectrum.

2.3. Previous work on cadmium stannate

Alnaimi and AL-Dileamy (2007) prepared TFs of Cd_2SnO_4 using thermochemical SPT at a temperature of 300-600 K for use in ordinary and thermal mirrors, highly specialized filters and solar cells. The precursor solutions used were cadmium II chloride pentahydrate dissolved in ethanol and tin II chloride trihydrate dissolved in acetic acid at a mole ratio of 2:1. The solution was left for 72 hours to ensure that the resulting solution was homogenous. The final solution was sprayed onto the preheated glass substrates. The mass method was used to calculate the thickness of the deposited TFs, which were observed to have a range within 300-600 nm. Values close to these had also been obtained earlier by Mott and Davis (1979). All the TFs formed were amorphous according to the X-Ray Diffraction (XRD) technique that was used to determine the film structure in the study, which was also in agreement with the work done by Clark (1980).

The type of electronic transition was determined by studying the UV-V spectrum in the wavelength range of 400-700 nm. An optimum band gap of 2.8-3.3 eV and a transmittance of 90% were obtained. They found out that the value of the band gap decreased as the film thickness increased, which they attributed to the increase in the thickness, leading to filling of structural gaps and hence, increasing localized states within the gap. Their finding agreed very well with the work done by Krishna et al (2010). The study did not dope the Cd_2SnO_4 with any material.

Krishna et al (2010) studied for the first time, the preparation of Cd_2SnO_4 TFs using low-cost homemade SPT at three different substrate temperatures of 400 °C, 450 °C and 500 °C for solar cell applications. The distance between the spray nozzle and the substrate (35 cm) and the spray angle (45 °) were kept constant. The carrier gas flow rate was kept at 61/min at a pressure of 6.5 x 10^4 Pa. The precursors used were cadmium acetate and tin II chloride solutions, mixed in the mole ratio of 2:1, 4:1 and 6:1 respectively. 3ml of 2M hydrochloric acid (HCl) was added in order to obtain a clear solution. This had also been done by Alnaimi and AL-Dileamy (2007).

TFs prepared at the substrate temperature of were amorphous, while those prepared at had the growth orientation along (1 1 1) in the orthorhombic structure. The sheet resistance of 160 Ω/ square was obtained for the TFs prepared without an additional layer. The process of formation of an additional layer reduced the sheet resistance to 15 Ω/ square but did not affect the optical and structural properties of the TFs. An optical transmittance of 91.7-99.8% was obtained for amorphous TFs of thickness of 160 nm in the wavelength range of 770-795 nm, which occurred at a temperature of 450 °C. Their findings agreed very well with those done by Bright (2013).

All the films prepared had a band gap of 2.9 eV without post-heat treatment, which was echoed later by Eman (2014). The film thickness was estimated using the gravimetric method. Computer controlled Phillips X-Pert Pro XRD was used to record the XRD pattern of the TFs using CuKα radiation of wavelength 1.5405 Å. The optical spectrum was recorded using Shimadzu UV-1601 in the wavelength range of 300-1100 nm (Krishna et al, 2010). The research also did not use any material for doping.

Eman (2014) studied the optical and electrical properties of Cd_2SnO_4 TFs deposited by Vacuum Evaporation Technique (VET) on glass substrates at room temperature. Films of thickness in the range of 300-600 nm were obtained. The Cd_2SnO_4 were evaporated using Edward (E306A) coating system under a vacuum of 2×10^{-5} mbar from the Cd_2SnO_4 powder that was 99.999% pure. The TFs were deposited on 7059 corning glass substrates at room temperature. The XRD studies showed that the films formed were polycrystalline in nature, with cubic structure and strong peaks in the direction (3 1 1). The intensity of the peaks increased with an increase in the film thickness, which he attributed to the increase in the grain size of the films. The grain size obtained varied between 19.1-21.4 nm, which increased with an increase in the film thickness from 300 to 600 nm.

The optical transmittance was measured using the UV-V-NIR spectrophotometer in the wavelength range of 200-1100 nm. A maximum transmittance of 70% in the visible spectrum and a band gap energy of 3.0 eV were obtained, both of which increased with increase in film thickness. They attributed the increase in both the transparency and band gap to the increase in the crystallization of film structure by increasing the grain size. Almost similar results had also been obtained earlier by Mohammad and Ghafor (1989). The research also did not use any material for doping.

Patil et al (2012) prepared TFs of both pure and Zn-doped Cd_2SnO_4 by SPT for the detection of chemical warfares. The precursors used were 0.1M cadmium nitrate tetrahydrate and 0.1M tin IV chloride pentahydrate at a mole ratio of 1:1. The dopant (Zn) was added to the mixture as zinc nitrate trihydrate at 5% by composition and then sprayed onto glass substrates at a temperature of 300 °C. All the TFs had a thickness of less than 100 nm. The structural properties of the deposited TFs were studied by XRD. The TFs formed were found to be orthorhombic. The Zn-doped TFs did not show any peak corresponding to the zinc, which they attributed to the very low content of Zn in the Cd_2SnO_4.

Both the pure and Zn-doped Cd_2SnO_4 TFs were tested against the stimulants of chemical warfare agents. The Zn-doped Cd_2SnO_4 TFs showed better sensing performance towards the stimulants (stimulant resin of 16 at 350 °C) as compared to the undoped TFs (stimulant resin of 5 at 350 °C). They explained the observation that ionic radius of zinc ion (Zn^{2+}) (0.073 nm) is almost similar to that of tin IV ion (Sn^{4+}) (0.071 nm) and smaller than that of cadmium II ion (Cd^{2+}) (0.095 nm), so that it can be incorporated into the Cd_2SnO_4 lattice easily by substituting for Sn^{4+} or Cd^{2+}. Zn as a dopant results in the surface modification and the formation of more oxygen vacancies, which can facilitate the enhancement of gas-sensing properties. It may be due to an ability of Zn ion to substitute Sn/Cd ions easily.

Cristaldi et al (2012) doped Cd_2SnO_4 with Y and studied the structural, electrical and electronic properties of the TFs of the Y-doped Cd_2SnO_4. The films formed were crystalline, with orthorhombic structure. The resulting films were characterized using XRD, atomic force microscope (AFM) and X-ray photoelectron spectroscope (XPS). The resulting values confirmed that Y doping causes a decrease in the grain dimension being 84 ± 6 and 61± 5 nm for the pure and the doped TFs respectively. The electrical measurements showed that the carrier concentration of the Y doped TFs increased by an order of magnitude compared to the undoped TFs. Although the study used a metal (Y) for doping, it did not study the optical properties of the Y-doped TFs.

Bhuvaneswari and Velusamy (2013) deposited TFs of fluorine-doped Cd_2SnO_4 on Corning 1737 glass substrates at a temperature of 540 °C by SPT using a temperature controller of accuracy of ±5 °C as a potential candidate for PV applications. The precursors used were 0.16M cadmium acetate and 0.02M tin II chloride. 3ml of 2M hydrochloric acid (HCl) was then added to the mixture in order to obtain a clear solution. The doping was done by adding ammonium fluoride at 0-5% weight of the total weight of the solution. Compressed air at about was used as the carrier gas.

The parameters such as the distance between the spray nozzle and the substrate (35 cm), spray angle (about 45.1 °C), spray duration (3s) and spray interval (30 s) were kept constant. The XRD measurements showed that the TFs were crystalline, with cubic structure and growth orientation along (2 2 2) direction. They observed that the intensity of the peaks decreased with increase in the fluorine doping concentration, likewise to the crystallite size from 17.8 to 47.1 nm, which is in line with the work done by Patil et al (2012).

Transmittance was measured in the wavelength range of 300-1100 nm. The average optical transmittance in the visible region (500-850 nm) increased from 79-83% after doping, with the band gap increasing from 2.8-3.23 eV for the 1% fluorine doping, then decreased to 3.18 eV with 5% fluorine doping. They attributed the shift of the band gap to the Burstein-Moss shift. The general increase in transmittance and band gap energy after doping had also been published earlier by Patil et al (2012). The research used chlorine, a non-metal for doping.

Both high transmittance of 80% and above (Kolokowsky and Davis, 2009) and a large band gap of 3.2 eV and above (Siefert, 1984) are among the desirable TCO material properties for use in TF PV solar cells, LCD screens and smartphone touchscreens. Doping of TCOs with non-metals raises the band gap as well as improving the transparency. Doping of TCOs with metals, on the other hand, lowers the band gap by introducing free charge carriers into the material. The presence of free charge carriers lowers the transmittance due to carrier absorption and scattering. Cd_2SnO_4 is a large band gap semiconductor with a band gap value of as high as 4.6 eV (Dawar and Joshi, 1984). This makes it very transparent, but poor electrical conductor (TCOs should have both high transmittance as well as good electrical conductivity). Doping the TFs of Cd_2SnO_4 with a metal lowers the band gap (improves the electrical conductivity), but also reduces the transparency. A balance, therefore, has to be made between the two. It was within this context that a metal (Fe) was chosen as the dopant and we investigated the optical properties of the deposited TFs with respect to concentration of the reactants (cadmium and tin) and deposition temperature within the spectral wavelength of 300-1100 nm to provide insight into the influence of Fe (metal) doping on the optical properties.

2.4. Thin film optics

Optical transitions start in semiconductors when the energy of photons is absorbed in a quantity equal to or higher than the forbidden band gap (Grove, 1967). When the required energy is almost equal to the difference between the lowest level of the CB and the highest level of the VB, electrons will transfer from VB to CB. The relationship between the intensity of the incident light I_o and the intensity of the transmitted light I_T is represented by an exponential of the form (Hummel, 2001):

$$I_T = I_0 \exp(-\alpha t), \quad (2.1)$$

where α is the absorption coefficient and t is the film thickness. According to equation (2.1), the optical absorption coefficient of TFs can be evaluated from the transmittance data using the relation (Eman, 2014):

$$\alpha = \frac{A}{t}, \; A = \alpha t, \quad (2.2)$$

where A is the absorbance and t is the film thickness in cm.

The absorbance A is given by $A = \ln\left(\frac{1}{T}\right)$, where T is the transmittance. Thus,

$$\alpha = \frac{-\ln(T)}{t}, \quad (2.3)$$

$$\text{where } T = \frac{I_T}{I_0}, \text{ the transmittance} \quad (2.4)$$

In terms of transmittance and reflectance (R), the absorption coefficient can also be given by the relation:

$$\alpha = \frac{-\ln\left(\frac{T}{1-R}\right)}{t} \quad (2.5)$$

Extinction coefficient *k* is given by:

$$k = \frac{\alpha\lambda}{4\pi}, \qquad (2.6)$$

where λ is the wavelength.

Refractive index of TFs can be given by the formula (Sakthivel et al, 2018):

$$n = \left(\frac{1+R}{1-R}\right) + \sqrt{\frac{4R}{(1+R)^2} - k^2} \qquad (2.7)$$

The optical band gap is the minimum energy needed to remove an electron from its bound state within an atom to its free state (from VB to CB). It is the energy difference between the VB and the CB. The band gap can either be direct or indirect. According to Ellingson and Heben (2011), a direct band gap is given by:

$$\alpha E = \chi(E - E_g)^{1/2}, \text{ from which we get: } (\alpha E)^2 = \beta(E - E_g). \qquad (2.8)$$

For indirect band gap, we have:

$$\alpha E = \chi(E - E_g)^2, \text{ from which we get: } (\alpha E)^{1/2} = \beta(E - E_g), \qquad (2.9)$$

where $\boldsymbol{\chi}$ is a constant and β = χ^2, hυ is the energy of the incident photon (h is the Plank's constant and υ is the frequency), E_g is the optical band gap and r is an index which can take different values according to electronic transition. The relations in equations 2.8 and 2.9 above are known as the *Tauc* relation (Marozau, 2009).

When a graph of $\alpha E^{1/r}$ against photon energy (E**)** is plotted, extrapolation of the linear portion of the plot to the energy axis at $(\alpha E)^{1/2} = 0$ (x-axis) for an indirect band gap or at $(\alpha E)^2 = 0$ for a direct band gap yields the optical band gap values of the deposited TFs (Makori et al, 2014).

Of the total radiation energy incident on an object, a fraction R is reflected from the top surface and a fraction T is transmitted through the bottom surface. The remaining fraction is lost through electronic absorption A processes and through scattering S at surface and volume imperfections (figure 2.2) (Ohring, 1992).

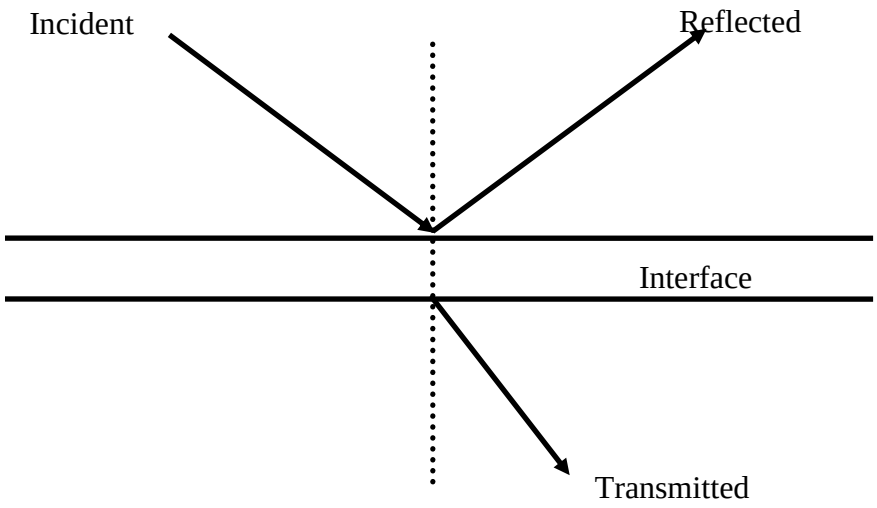

Figure 2.2: Light interaction with a material medium

Adding the various contributions above give unity (Ohring, 1992):

$$R + T + A + S = 1. \qquad (2.10)$$

Of the terms in equation (2.10) above, T and R are of the greatest interest to the study of optical properties.

The incident photon energy E (in eV) can be calculated from the relation:

$$E\ (eV) = hv = \frac{1.24}{\lambda\ (\mu m)} \qquad (2.11)$$

The determination of the structure of a crystal can be understood by Bragg's law (Meyers, 1990), given as:

$$n\lambda = 2d_{hkl}sin\theta, \quad (2.12)$$

where n is an integer (layer number), λ is the wavelength of the X-ray used, θ is the diffraction angle and hkl are the Miller indices. Rearranging equation 2.12 gives the interplanar distance d_{hkl} as:

$$d_{hkl} = \frac{n\lambda}{2\sin\theta} \quad (2\ 13)$$

The lattice parameter for a cubic cell is given as (Warren, 1999):

$$\frac{4sin^2\theta}{\lambda^2} = \frac{1}{d_{hkl}^2} = \frac{h^2+k^2+l^2}{a^2} \quad (2.14)$$

Rearranging equation 2.14 gives the expression for the lattice parameter a as:

$$a = \sqrt{d^2(h^2 + k^2 + l^2)} \quad (2.15)$$

For an orthorhombic unit cell, the equation relating the lattice parameters a, b and c is (Yang et al, 2006):

$$\frac{1}{d_{hkl}^2} = \frac{h^2}{a^2} + \frac{k^2}{b^2} + \frac{l^2}{c^2} \quad (2.16)$$

Finding the values of a, b and c involve identifying three known peaks (indexed peaks, hkl) and using them to form three simultaneous equations. Solving the simultaneous equations gives the values of the parameters in angstrom (Å).

The unit cell volume of the cubic unit cell is given by (Cullity and Stock, 2001):

$$V = a^3 \quad (2.17$$

For the orthorhombic unit cell, the volume is given by:

$$V = abc \quad (2.18)$$

2.5. Thin film applications

TFs are made by depositing one or more thin layers on a substrate. The substrate can be glass, plastic or metal (Green, 2003). The TFs have wide applications. Some of the current applications include touch screens, TF solar cells, LEDs, TF batteries, window films and heat mirrors (Siefert, 1984).

2.5.1. Thin film photovoltaic cells

TF PV cells, also known as TF solar cells, are second generation solar cells made of film thicknesses ranging from a few nanometers to tens of micrometers. They are much thinner than the first-generation crystalline silicon (c-Si) solar cells that use wafers of as thick as 350 μm. Because they are thin, the TF PV cells are flexible, lighter and have less friction. The PV cells are used in building integrated photovoltaics and rigid TF solar panels (Pearce and Lau, 2002).

Some of the current TF solar cells have high efficiencies of up to 21%, outperforming the dominant c-Si solar cells at 20.4% (Ayre, 2014). However, the lifespan of these TF solar cells is still an issue. They degrade relatively faster compared to the c-Si cells, with a lifespan of less than 20 years (Green, 2007). TF solar cells mainly require TFs with a transmittance of above 80%, a large absorption coefficient in the order of x 10^4 cm^{-1} and a band gap of above 3.2 eV in order to avoid absorption of light in most of the solar spectrum (Siefert, 1984).

2.5.2. Liquid Crystal Displays (LCDs)

The LCDs are flat-panel displays that use the light modulating properties of liquid crystals. The glass at the front of the panel (in between the polarizing filter and the liquid crystal) is mainly made of ITO, which has been criticized for its high cost and scarcity (Mazzeo et al, 2013). LCDs are normally used to create digital displays in many devices, including television screens, computer monitors, smartphone touch screens, handheld game consoles and personal digital assistants (Chang and Hong, 2013).

2.5.3. Window films

Window films are TFs of a laminate. They can be installed to the interior of glass surfaces; usually in homes, buildings and automobiles. The film is usually made from polyester due to its clarity, tensile strength, dimensional stability and the ability to accept a variety of surface-applied or embedded treatments. The film is made such that it allows part of the electromagnetic waves to pass through but blocks others. An example is a film used to keep the rooms at a fairly constant temperature. These films allow all the other rays to pass through the window but block the IR (DeBusk, 2015).

Some window films are also made in such a way that they are transparent on one side but translucent on the other side. This is made possible by coating the window with a thin layer that allows transmission of the visible portion of the electromagnetic spectrum in one direction only. Such films can be used in the window panes in houses and toilet windows (Tam and Stockton, 2012).

CHAPTER THREE
MATERIALS AND METHODS

3.1 Introduction

This chapter presents the materials and methods that were used in preparing and depositing the TFs of Cd_2SnO_4 in this study. It focuses on the cleaning of the glass substrates that were used as the target, the preparation of the precursor solutions used and the deposition of the TFs. The parameters that were kept constant in the experiment and the measurements that were made are also discussed here.

3.2 Substrate cleaning

There are many methods that can be used to clean glass substrates. The one that was chosen for this research is the Aqua Regia. The Aqua Regia method was chosen because it produces very clean surfaces, which are free from solvents or traces of metals (Shugar and Ballinger, 1996). Microscope glass slides of dimensions 25.4 mm by 76.2 mm by 1.1 mm were used as the substrates.

While wearing acid-proof gloves, safety goggles and a lab coat, the Aqua Regia was prepared by mixing stock solutions of HCl and nitric (V) acid (HNO_3) at a ratio of 3:1 by volume, that is: 600ml of stock solution of HCl and 200ml of stock solution of HNO_3 in a polypropylene container, giving a total volume of 800ml of the final solution mixture. This was done in the open air in order to avoid poisoning by chlorine and nitrosyl chloride gases that fume from the Aqua Regia.

The glass slides were then put into the mixture in the polypropylene container to soak for 12 hours (overnight), then removed from the Aqua Regia solution and rinsed in deionized (DI) water. Whatman lens cleaning tissues, model number 105 (100 x 150 mm) were used to wipe the glass slides dry. After cleaning, the Aqua Regia solution was neutralized by sodium hydroxide solution. The neutralized solution was then discarded.

It took two hours to clean all the 100 glass slides that were used in this study. The clean glass slides that were now ready for deposition were kept in the slide holder. The scheme in figure 3.1 shows the cleaning process.

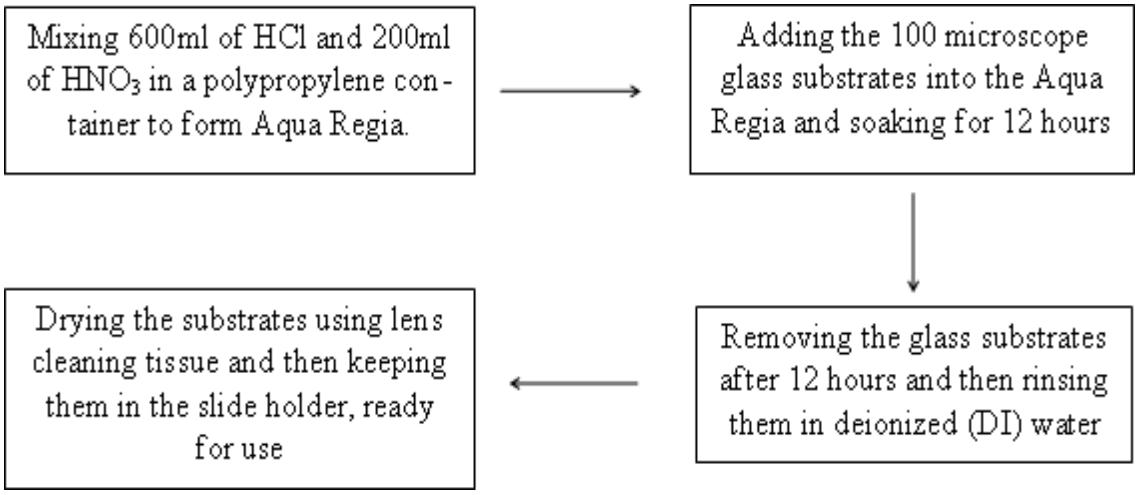

Figure 3.1: The process of cleaning the glass substrates

3.3 Preparation of solutions

The masses of the solids (cadmium acetate, tin II chloride and iron III chloride) that were dissolved in the solvent to form the solutions for spraying were determined using the following procedure:

$$Moles = molarity\ x\ volume$$

Since the volumes of the solutions to be sprayed were to be 250 ml and at a concentration of 0.1M, the number of moles was found to be:

$$Moles = 0.1\ x\ \left(\frac{250}{1000}\right) = 0.025\ moles$$

The mass of individual solids to be weighed were found by:

$$Mass = moles\ x\ molar\ mass$$

For cadmium acetate dihydrate, the molar mass is 266.53, which gave the mass as:

$$Mass = 0.025\ x\ 266.53 = 6.67g$$

For tin II chloride dihydrate, the molar mass is 225.63, which gave the mass as:

$$Mass = 0.025\ x\ 225.63 = 5.64g$$

For iron III chloride, the molar mass is 162.2, which gave the mass as:

$$Mass = 0.025\ x\ 162.2 = 4.06g$$

The masses of the 0.2M and 0.3M concentrations of cadmium acetate dihydrate and tin II chloride dihydrate were obtained as multiples of the masses of the 0.1M concentrations.

Mettler Toledo PB303 weighing balance was then used to accurately weigh the masses of the compounds that were dissolved in the solvent (99.99% pure ethanol) in order to form the solutions for spraying. The aqueous solution of cadmium acetate was prepared by dissolving the 6.67g (99.99% pure) of the compound in 250 ml of ethanol in a 250 ml volumetric flask. This made the 0.1M solution. 250 ml of 0.2M (13.33g) and 0.3M (20.00g) were prepared in different flasks. The aqueous solution of tin II chloride was prepared by dissolving the 5.64g (99.99% pure) of the compound in 250 ml of ethanol in a 250 ml volumetric flask. This made the 0.1M solution. 250 ml of 0.2M (11.28g) and 0.3M (16.92g) were prepared in different flasks. The dopant was prepared by dissolving the 4.06g of iron III chloride (99% pure) in 250 ml of ethanol in a 250 ml volumetric flask. This made the 0.1M solution. All the three chemicals (cadmium acetate, tin II chloride and iron III chloride) were manufactured by Central Drug House (CDH) (P) Ltd. 7/28 Vardaan House, Daryaganj, New Delhi-110002 (India).

The different concentrations of cadmium acetate and tin II chloride were then mixed (10 ml of each, giving a total volume of 20ml) in the ratio of 0.1:0.1, 0.2:0.2 and 0.3:0.3 (0.1M cadmium acetate: 0.1M tin II chloride, 0.2M cadmium acetate: 0.2M tin II chloride and 0.3M cadmium acetate: 0.3M tin II chloride) respectively, forming a white precipitate. 3 ml of HCl (2M) was then added to the white precipitate, after which it dissolved to form a colourless solution of Cd_2SnO_4 (Krishna et al, 2010).

The different mixtures of the colourless solution (now Cd_2SnO_4), were finally mixed with the dopant at 0-8% by volume of Cd_2SnO_4 solution. Tables 3.1, 3.2 and 3.3 show the ratios of mixing the solutions and the number of the glass substrates onto which the solution mixtures were sprayed.

Table 3.1: Cadmium acetate and tin II chloride at a mole ratio of 0.1:0.1M by concentration, then adding iron III chloride at 0-8% by volume of the Cd_2SnO_4 solution

$Cd(CH_3COO)_2$	$SnCl_2$	$\%FeCl_3$	Vol. of $FeCl_3$ (ml)	No. of slides
0.1	0.1	0	0.0	4
0.1	0.1	2	0.4	4
0.1	0.1	4	0.8	4
0.1	0.1	8	1.6	4

Table 3.2: Cadmium acetate and tin II chloride at a mole ratio of 0.2:02M by concentration, then adding iron III chloride at 0-8% by volume of the Cd_2SnO_4 solution

$Cd(CH_3COO)_2$	$SnCl_2$	$\%FeCl_3$	Vol. of $FeCl_3$ (ml)	No. of slides
0.2	0.2	0	0.0	4
0.2	0.2	2	0.4	4
0.2	0.2	4	0.8	4
0.2	0.2	8	1.6	4

Table 3.3: Cadmium acetate and tin II chloride at a mole ratio of 0.3:0.3M by concentration, then adding iron III chloride at 0-8% by volume of the Cd_2SnO_4 solution

$Cd(CH_3COO)_2$	$SnCl_2$	$\%FeCl_3$	Vol. of $FeCl_3$ (ml)	No. of slides
0.3	0.3	0	0.0	4
0.3	0.3	2	0.4	4
0.3	0.3	4	0.8	4
0.3	0.3	8	1.6	4

3.4 Deposition

Spray Pyrolysis Equipment (model number HO-TH-04) with a temperature controller of accuracy of ±7 °C was used for spraying in the study. The final solutions (at different concentrations) were poured into the syringe pump (gun) at a time and then sprayed onto the preheated glass substrates that were kept at a constant temperature of 450 °C to obtain the Cd_2SnO_4 TFs (figure 3.2). For every combination of the mixture and at the constant temperature of 450 °C, say 0.1M cadmium acetate, 0.1M tin II chloride and 0% iron, four glass substrates were sprayed at once. More films at the concentration of 0.1:0.1 were also prepared at substrate temperatures of 400 ^oC and 350 ^oC.

Figure 3.2: The deposition process

3.5 Variables

Photon wavelength was the independent variable in the study, while the direct and measurable dependent variables were the optical transmittance and reflectance. The deposition temperature was varied from 350 °C to 450 °C in steps of 50 °C. That is 350 °C, 400 °C and 450 °C.

The spray duration was kept constant at 2 minutes (Table 3.6). The different concentrations of the solution mixtures at the three deposition temperatures were thus deposited for a time of two minutes. Table 3.4 shows the parameters that were kept constant during spraying.

Table 3.4: Parameters that were kept constant during spray deposition

Spray duration	2 minutes
Air	on
Flow rate	2 ml/ min
Flow factor	1
Spray angle	90 °C
Distance between spray nozzle and target	35 cm

After deposition, the TFs were taken for measurements of transmittance, reflectance, film thickness, structure and chemical composition.

3.6 Measurements

3.6.1 Mass, transmittance and reflectance

The measurement of the masses of cadmium acetate, tin II chloride and iron III chloride that were dissolved in ethanol to form the spray solutions were made using the Mettler Toledo PB303 analytical balance of accuracy 0.001g and a maximum capacity of 310g.

The measurements of transmittance and reflectance were made using the Shimadzu Solid Spec 3700 Deep Ultraviolet Spectrophotometer in the wavelength range of 300-1100 nm in steps of 1 nm. The spectrophotometer had an accuracy of ± 0.3 nm in the UV-VIS wavelength region and ± 0.32 nm in the NIR region, with a resolution of 0.1 nm. The sample was illuminated with light from a 50W halogen lamp.

3.6.2 X-Ray diffraction and chemical composition

The XRD analysis was done using Phillips X-Ray diffractometer system with CuK_α source of wavelength of 1.540598 Å. The analysis was done through an angle of 2θ ranging from 5^o to 90^o in steps of 0.05^o.

The chemical composition of the TFs was determined by XPS, ESCALAB 250 Xi, Thermo-Fisher Scientific with an accuracy of 1000 ppm. Monochromatic Al-Kα radiation of energy of 1486.6 eV was used as the excitation. Table 3.5 shows the XPS chemical analysis data for Cd_2SnO_4.

Table 3.5: XPS surface analysis data for Cd_2SnO_4.

Peak	Atomic concentration (%)	Weight concentration (%)
Cd	28.57	55.10
Sn	14.29	28.94
O	57.14	15.32

The data in table 3.5 (weight concentration) was used to calculate the empirical formula of the compound as shown in table 3.6.

Table 3.6: Determination of the empirical formula of the deposited cadmium stannate

Atom	Cd	Sn	O
% by mass	55.10	28.94	15.32
Molar mass	112.411	118.710	15.999
Moles	55.10/112.411 =0.4902	28.94/118.710 =0.2438	15.32/15.999 =0.9576
Mole ratio	0.4902/0.2438 =2.010 =2	0.2438/0.2438 =1.000 =1	0.9576/0.2438 =3.928 =4

Table 3.6 shows that the ratio of Cd: Sn: O is 2:1:4. Thus, the chemical formula of the deposited TFs is Cd_2SnO_4.

3.6.3 Film thickness

The measurement of film thickness was made using the computerized KLA-tensor alpha-step IQ surface profiler with a resolution of 0.014 µm and a thickness range of 8 nm-2 mm step heights with an accuracy of 0.75 nm. The profiler characterized the surface by scanning with a diamond-tipped stylus from the bare portion of the TF to the coated portion.

The thicknesses that were measured for both the undoped and the doped TFs are presented in tables 3.7 and 3.8.

Table 3.7: Thicknesses of Cd_2SnO_4 TFs at different concentrations deposited at a temperature of 450 °C

Concentration (M)	0.1:0.1	0.2:0.2	0.3:0.3
Thickness (nm)	76.0 (0% Fe)	110.1 (0% Fe)	118.1 (0% Fe)
	76.4 (2% Fe)	116.0 (2% Fe)	139.1 (2% Fe)
	80.2 (4% Fe)	121.3 (4% Fe)	158.4 (4% Fe)
	88.2 (8% Fe)	127.0 (8% Fe)	176.3 (4% Fe)

Table 3.8: Thickness of 0.1: 0.1M Cd_2SnO_4 TFs deposited at the three temperatures

Temperature (°C)	450	400	350
Thickness (nm)	76.0 (0% Fe)	83.4 (0% Fe)	86.5 (0% Fe)
	76.4 (2% Fe)	85.8 (2% Fe)	87.2 (2% Fe)
	80.2 (4% Fe)	87.3 (4% Fe)	89.1 (4% Fe)
	88.2 (8% Fe)	90.1 (8% Fe)	94.0 (4% Fe)

CHAPTER FOUR
RESULTS AND DISCUSSION

4.1 Introduction

The results obtained in this study are presented in this chapter. The samples of Cd_2SnO_4 were prepared at different concentrations and also at different deposition temperatures and their optical properties pointed out and discussed under these conditions in the wavelength range of 300-1100 nm. The direct measurable quantities: transmittance and reflectance were measured, from which the optical constants: absorption coefficient, extinction coefficient, refractive index and band gap were determined. The XPS, as well as the XRD analyses of the deposited TFs, are also presented and discussed in this chapter.

4.2 X-Ray photoelectron spectroscopic studies

The intensity against binding energies for Cd, Sn, O and Fe were plotted to obtain figure 4.1.

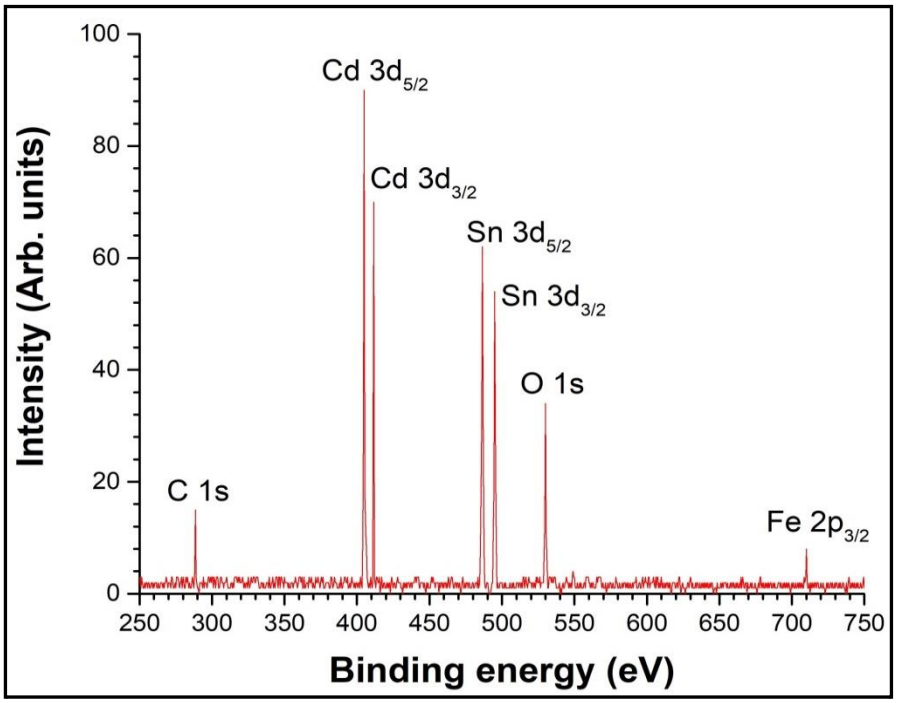

Figure 4.1: Binding energies for cadmium, tin, oxygen and iron

Figure 4.1 shows that the XPS spectra contained characteristic peaks of Cd, Sn, O, Fe and a weak peak of Carbon (C) at 288 eV. The peak for C can be attributed to the contamination in the samples. The weak peak of C has also been reported by Jianchao et al (2018) at an energy of 289 eV.

The binding energy for Cd $3d_{5/2}$ was found to be 404.71 eV while that of Cd $3d_{3/2}$ was found to be 411.52 eV, indicating that Cd was in the Cd^{2+} bonding state. The spin-orbit splitting between Cd $3d_{3/2}$ and Cd $3d_{5/2}$ was found to be 6.81 eV. The binding energy for Sn $3d_{5/2}$ was found to be 495.18 eV while that of Sn $3d_{3/2}$ was found to be 486.55 eV, indicating that the Sn was in the Sn^{4+} bonding state. The spin-orbit splitting between Sn $3d_{3/2}$ and Sn $3d_{5/2}$ was found to be 8.63 eV. The binding energy for O 1s was found to be 530.05 eV. The values of the binding energy obtained from the XPS analysis in this study are in agreement with those of Golestani-Fard and Mackenzie (1983), who obtained a value of 531.2 eV for O 1s, 404.7 eV for Cd $3d_{5/2}$ and 486.2 eV for Sn $3d_{5/2}$. The binding energy values obtained in this study are typical of Cd_2SnO_4 (Cristaldi et al, 2012).

The binding energy for Fe was detected with a weak intensity, which occurred only in the doped TFs, with a value of 710.2 eV, which indicates a bonding state of Fe^{3+}. The weak Fe peak in the doped TFs is due to the low concentration of Fe in the starting solution.

4.3 X-Ray diffraction studies

The XRD studies of the TFs are shown in figure 4.2.

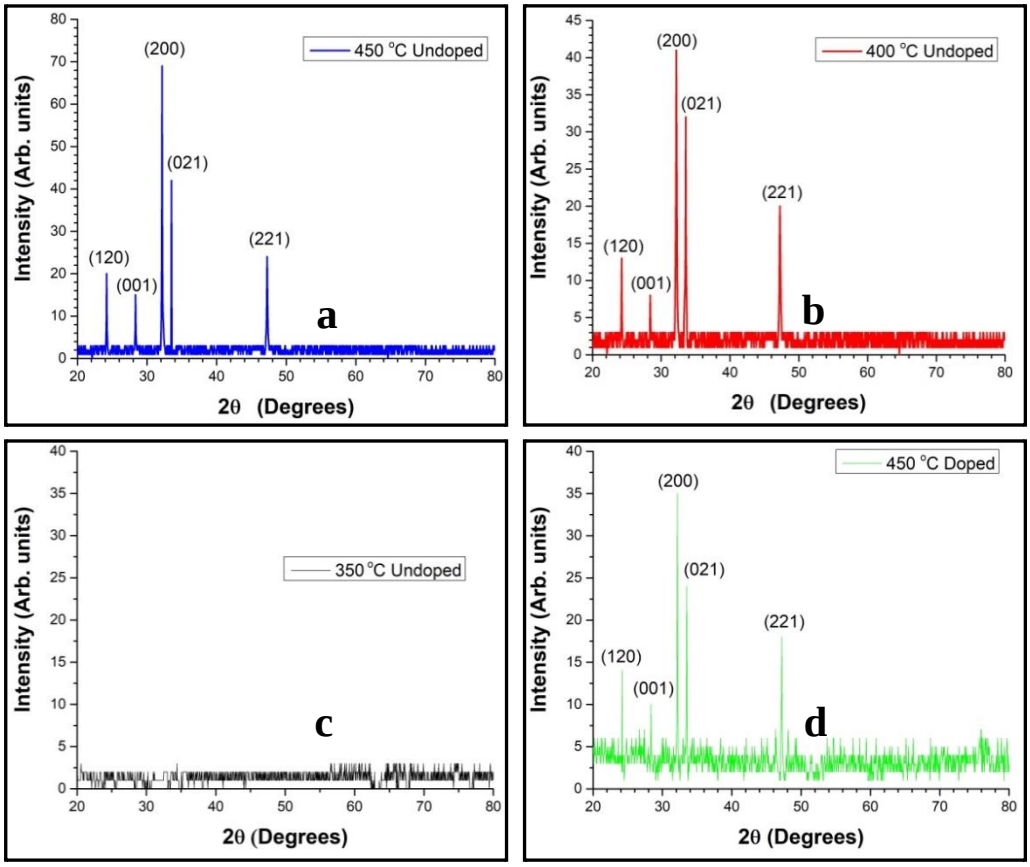

Figure 4.2: X-Ray diffraction studies on Cd_2SnO_4

The intensity of the peaks increased with an increase in the deposition temperature (figure 4.2a and b). This can be attributed to the improvement in the crystallinity with deposition temperature. Long and Cheng (2012), who studied the properties of ITO, also observed the increase in the intensity of the peaks with an increase in the deposition temperature, which they attributed to the increase in the crystallinity of the deposited TFs.

The TFs deposited at 350 °C were amorphous as can be observed in figure 4.2c. The crystalline TFs had growth orientation along the (2 0 0) direction in the orthorhombic structure (figure 4.2a, b and d), which is in agreement with the findings of Krishna et al (2010), who observed that the TFs of Cd_2SnO_4 are orthorhombic with growth orientation along the (1 1 1) direction. Chopra et al (1983) also reported the orthorhombic structure of Cd_2SnO_4.

The peaks (1 2 0), (0 0 1), (2 0 0) (0 2 1) and (2 2 1) in figure 4.2 correspond to angles 2θ = 24.25° (24.20°), 28.40° (28.35°), 32.20° (32.15°), 33.55° (33.50°) and 47.25° (47.20°) respectively, giving d_{hkl} spacing (interplanar distance) values shown in table 4.1, which were calculated using equation 2.13.

Table 4.1: d spacings for the strongest peaks

Sample	2θ (Degrees)	Peak	d_{hkl} (Å)
Cd_2SnO_4	24.25	(1 2 0)	3.6673
	28.40	(0 0 1)	3.1401
	32.20	(2 0 0)	2.7777
	33.55	(0 2 1)	2.6690
	47.25	(2 2 1)	1.9221
Cd_2SnO_4.Fe	24.20	(1 2 0)	3.6748
	28.35	(0 0 1)	3.1456
	32.15	(2 0 0)	2.7819
	33.50	(0 2 1)	2.6728
	47.20	(2 2 1)	1.9241

Doping did not change the structure of the TFs as can be observed in figure 4.2, although the doped TFs produced weaker peaks compared to the undoped TFs at the same deposition temperature (comparing figure 4.2a and d).

The reduction in the intensity of the peaks upon doping implies that crystallinity of the TFs decreased with doping, which implies that the crystallinity is deteriorated with poorly incorporation of Fe, which can be attributed to the Fe atoms being able to incorporate interstitially into the lattice of Cd_2SnO_4 instead of occupying the proper lattice positions. The poor incorporation of foreign bodies into the lattice of Cd_2SnO_4 has also been reported by Dislich and Hinz (1980). The poor incorporation causes a structural disorder, leading to a change in the interplanar distance d_{hkl} as can be observed in table 4.1.

The lattice parameters a, b and c of the deposited TFs were calculated using equation 2.16. The results are presented in table 4.2.

Table 4.2: Lattice parameters of the deposited Cd_2SnO_4 TFs

Parameter	a	b	c
Undoped (Å)	5.5554	9.7645	3.1766
8% doped (Å)	5.5638	9.7882	3.1856

The unit cell volumes of the TFs were calculated using equation 2.18. The undoped TFs gave a unit cell volume of 172.32 Å, while that of the 8% doped TFs gave 173.49 $Å^3$. The lattice parameters obtained in this study are in agreement with some of the previous work. Dawar and Joshi (1984) obtained the following values: a = 5.568 Å, b = 9.887 Å and c = 3.192 Å, with pbam space group (number 55) and a unit cell volume of 175.722 $Å^3$. Setty and Sinha (1986) obtained the lattice parameters of Cd_2SnO_4 as a = 5.546-5.684 Å, b = 9.869-9.888 Å and c = 3.189-3.193 Å, with a unit cell volume of 174.545-179.457 $Å^3$.

Jeyadheepan and Sanjeeviraja (2014) also reported the orthorhombic crystal structure of Cd_2SnO_4 with a pbam space group (number 55). They obtained the lattice parameters of a = 5.568(2) Å, b = 9.894(4) Å and c = 3.193(12) Å, with a unit cell volume of 175.96(10) $Å^3$ and density of 7.002 g/cm^3.

The lattice parameters of the doped TFs obtained in this study are higher than those of the undoped TFs (table 4.2), which confirm the interstitial incorporation of Fe into the lattice of Cd_2SnO_4 instead of occupying the proper lattice positions.

4.4 Effect of concentration of reactants

4.4.1 Transmittance

The measurements of transmittance were made in the UV-V-NIR wavelength range of 300-1100 nm. Figure 4.3 shows the transmittance obtained.

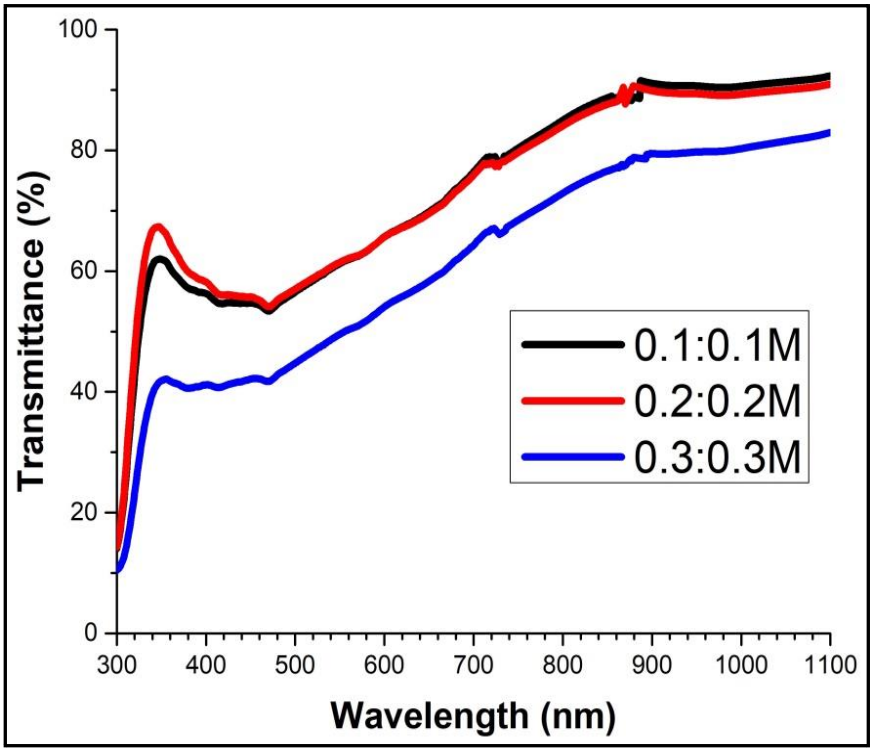

Figure 4.3: Transmittance of undoped Cd_2SnO_4 TFs at different concentrations

Figure 4.3 shows that transmittance increases with a decrease in the concentration of the starting solution. The concentration of 0.1:0.1M gave the highest transmittance of 78.45% at the upper end of the visible spectrum (700 nm). This is followed closely by the concentration of 0.2:0.2M, which gave 77.72% transmittance. The concentration of 0.3:0.3M gave the least transmittance of 64.27%. The decrease in transmittance with an increase in the concentration of reactants is due to an increase in the concentration of free carriers. Thus the effect of free carrier absorption reduced the transmission in the UV-V-NIR wavelength region.

The 78.45% value of transmittance for the TFs deposited at the 0.1:0.1M concertation is close to 80%, the recommended value for TCOs (Andreas, 2012). According to Grolik and Kopp (2003), transmittance is limited by among other factors, the reflectance. Thus, transmittance can never reach 100%

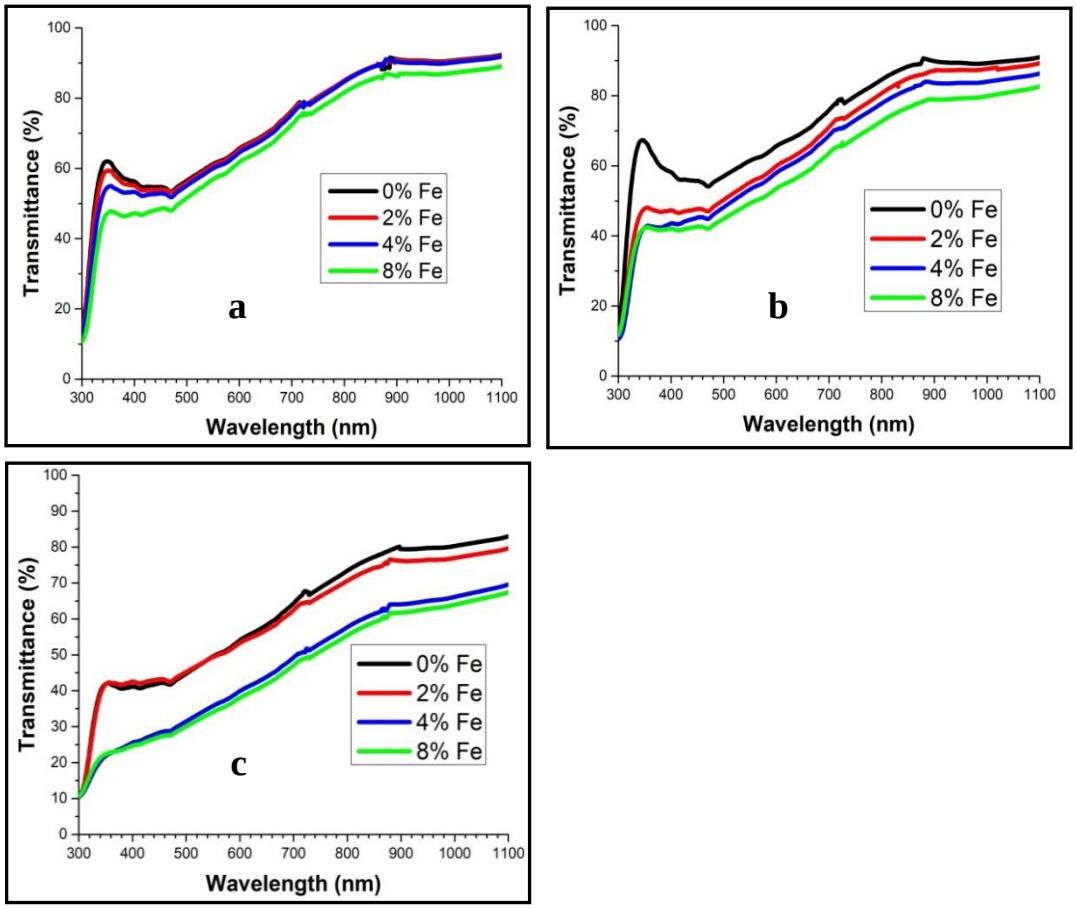

Figure 4.4: Transmittance of: (a) 0.1:0.1M Cd_2SnO_4, (b) 0.2:0.2M Cd_2SnO_4 and (c) 0.3:0.3M Cd_2SnO_4 with 0-8% Fe

There was negligible transmittance at short wavelengths below 300 nm. This is because most of the incident light is absorbed in this wavelength region, the region of fundamental absorption (Mulama et al, 2014). Rakesh et al (2018) also mentioned the low transmittance in the near UV region, which they attributed to be limited by the band gap, as photons with energy larger than the band gap are absorbed.

At the same deposition temperature of 450 °C, the dopant (Fe) was added to the Cd_2SnO_4 solution at the different concentrations. As can be observed in figure 4.4, introduction of the dopant reduced the optical transmittance of the deposited TFs. This is due to the absorption of the incident light by the free carriers. The decrease in transmittance of the TFs upon doping is in agreement with the results obtained by Maity and Chattopadhyay (2006), who attributed it to the defects of the dopant (aluminium) in the deposited TFs.

In figure 4.4, it is observed that the higher the concentration of the dopant, the lower the optical transmittance. This is because the higher the concentration of the dopant, the higher the number of free carriers introduced into the TFs and the higher the absorption of the incident light. All the graphs of 8% Fe in figure 4.4 have the lowest transmittance.

Samar et al (2016) who studied the optical properties of Fe-doped zinc oxide also observed that the average optical transmittance in the visible spectrum region of 300-1100 nm decreased consistently with increasing doping concentration, which they attributed to the increase in the surface roughness, promoting the increase of the surface scattering of light.

An increase in the concentration of the reactants lowers the transmittance, which is not a desirable trend for TCO materials, since TCOs should a high transmittance of $\geq$80%. Thus, the undoped TFs deposited at 0.1:0.1M produced the best transmittance for TCOs in this study.

4.4.2 Absorption coefficient

Absorption coefficient of the deposited TFs was determined using equation 2.3. Figure 4.5 shows that the absorption coefficient decreased with an increase in the wavelength, increasing sharply at short wavelengths below 350 nm. This implies that the absorption coefficient increased with a decrease in the transmittance, since the films become more absorbing at short wavelength range. The sharp increase in the absorption coefficient at short wavelength is because the short wavelength region is the region of fundamental absorption. Moreover, the short wavelength region is the band gap region, the region where the tightly bound electrons in the material become mobile and jump from the VB to CB. The free electrons then absorb more of the incident photon energy (Butcher and Pitt, 2009).

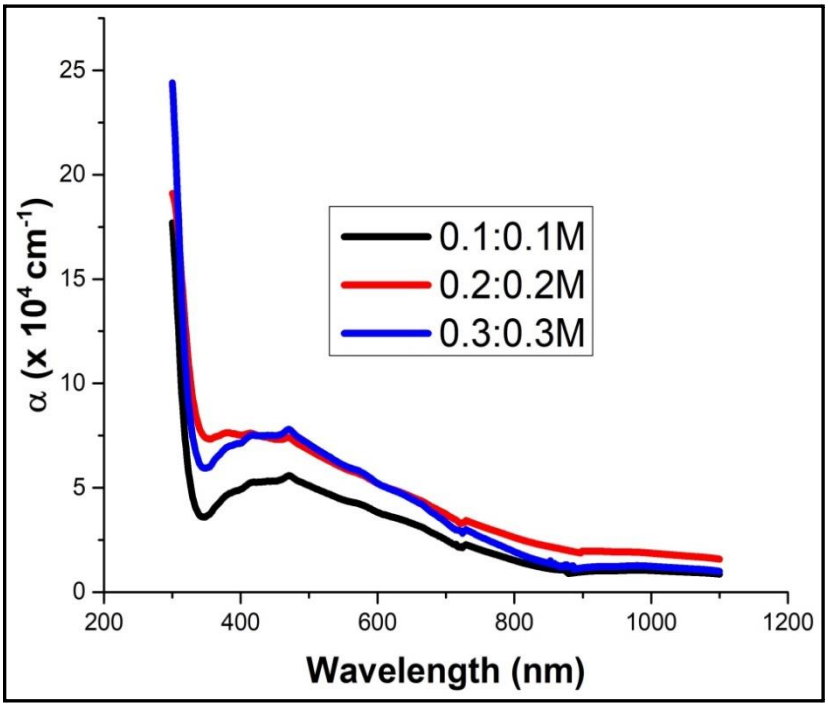

Figure 4.5: Absorption coefficient of undoped Cd_2SnO_4 TFs at different concentrations

Khusayfan and El-Nahass (2013) who studied the optical properties of ITO, also observed the drastic rise in the absorption coefficient of the deposited TFs in the UV region, which they attributed to excitations across the fundamental band gap. They asserted that the optical properties around the fundamental absorption edge are complicated by the occurrence of logarithmic band edges, with some weak absorption at the blue end of the luminous spectrum.

As can be observed in figure 4.5, absorption coefficient increased with increase in the concentration of the reactants. The TFs deposited at a concentration of 0.3:0.3M recorded the highest value of absorption coefficient of 5.50469 x 10^4 cm^{-1} at the 588nm wavelength, while those deposited at the 0.1:0.1M concentration produced the lowest value of 4.04401 x 10^4 cm^{-1}. The highest value of the absorption coefficient obtained for the TFs deposited at the 0.3:0.3M concentration is due to an increase in the number of particles deposited.

When the TFs were doped, the graphs in figure 4.6 were obtained. Figure 4.6 shows that the absorption coefficient of the doped TFs still increased with increase in the concentration of Cd_2SnO_4, just like those of the undoped TFs (figure 4.5). The increase in absorption coefficient with an increase in the concentration of the dopant is because the doped TFs absorb more of the incident light than the undoped ones, which can be attributed to the increase in the free carriers upon doping (Bushra and Shallal, 2014). The increase in absorption coefficient with doping concentration accompanies a decrease in the transmittance. The 8% doped TFs at a concentration of 0.3:0.3M recorded the highest absorption coefficient of 5.99479 cm^{-1}.

The same increase in the absorption coefficient of TFs upon doping has been reported by Samar et al (2016), who studied the optical properties of zinc oxide TFs. They attributed it to increase in the concentration of donor levels inside the energy gap near the conduction band. The donor concentration led to the absorption of photons with few energies and therefore, an increase in the values of the absorption coefficient, and the decrease in the band gap.

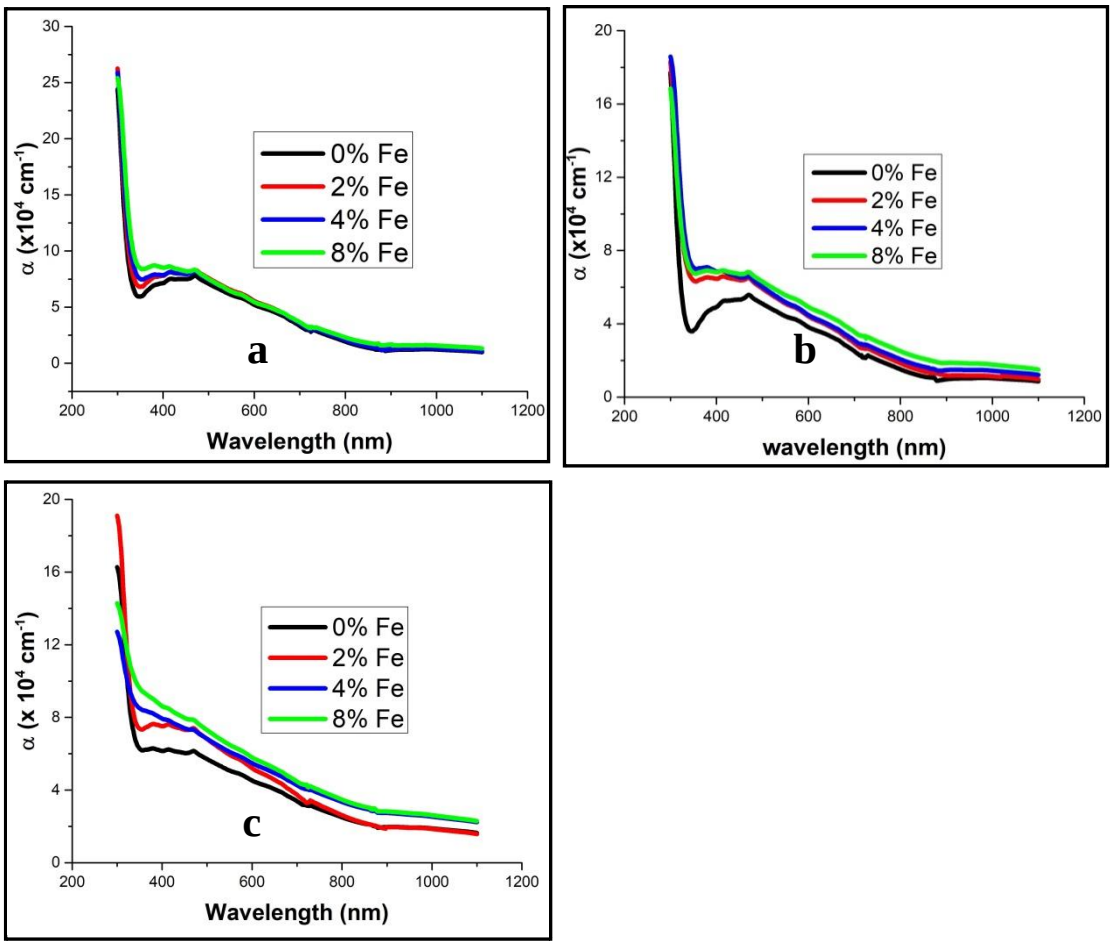

Figure 4.6: Absorption coefficient of (a) 0.1.0.1M Cd_2SnO_4, (b) 0.2:0.2M Cd_2SnO_4 and (c) 0.3:0.3M Cd_2SnO_4 with 0-8% Fe

Typical TCO materials have an absorption coefficient of greater than $x10^4$ cm^{-1} in the UV-V-NIR spectra (Coutts et al, 2000). The present study obtained values of absorption coefficient within the range of x 10^4 cm^{-1}, which is ideal for TCO materials.

4.4.3 Extinction coefficient

Extinction coefficients of the TFs were calculated using equation 2.6. As can be observed in figure 4.7, the extinction coefficients of the TFs were found to increase sharply at short wavelengths below 350 nm, the region of fundamental absorption. The extinction coefficient was also observed to increase with an increase in the concentration of the precursor solutions, which is due to the increase in the absorption coefficient, since absorption coefficient and extinction coefficient are directly related according to equation 2.6.

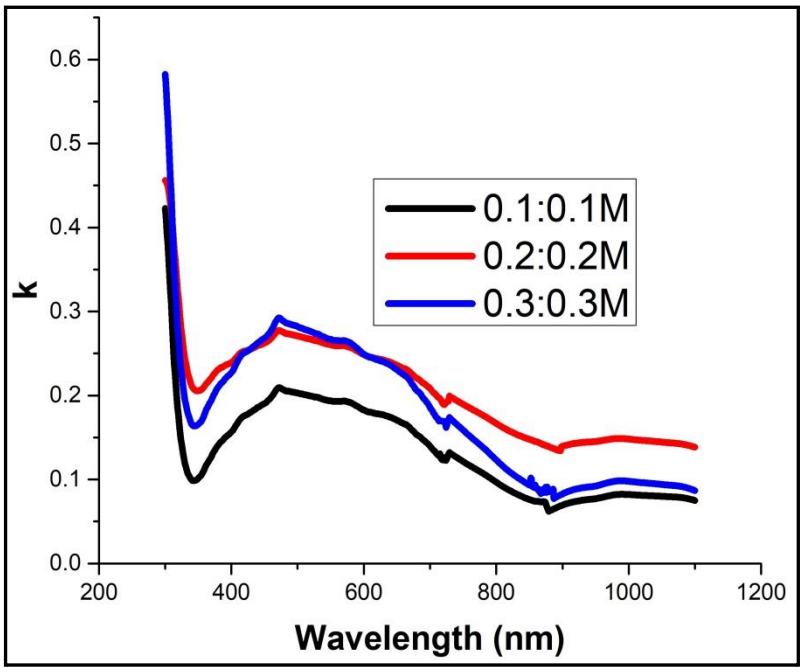

Figure 4.7: Extinction coefficient of undoped Cd_2SnO_4 TFs at different concentrations

The rise and fall in the absorption coefficient observed in the forbidden gap region in figure 4.7 is directly related to the absorption of light. The TFs deposited at a concentration of 0.1:0.1M had the lowest extinction coefficient of 0.18817 while those deposited at a concentration of 0.3:0.3M had the highest of 0.25754 at the wavelength of 588nm.

Upon doping (figure 4.8), the extinction coefficient was also observed to increase with an increase in the concentration of Cd_2SnO_4, same to those that were not doped (figure 4.7). However, the values for the doped TFs (figure 4.8) are higher than those for the undoped TFs (figure 4.7), increasing with the increase in the concentration of the dopant. The 8% doped TFs deposited at a concentration produced the highest extinction coefficient of 0.28047.

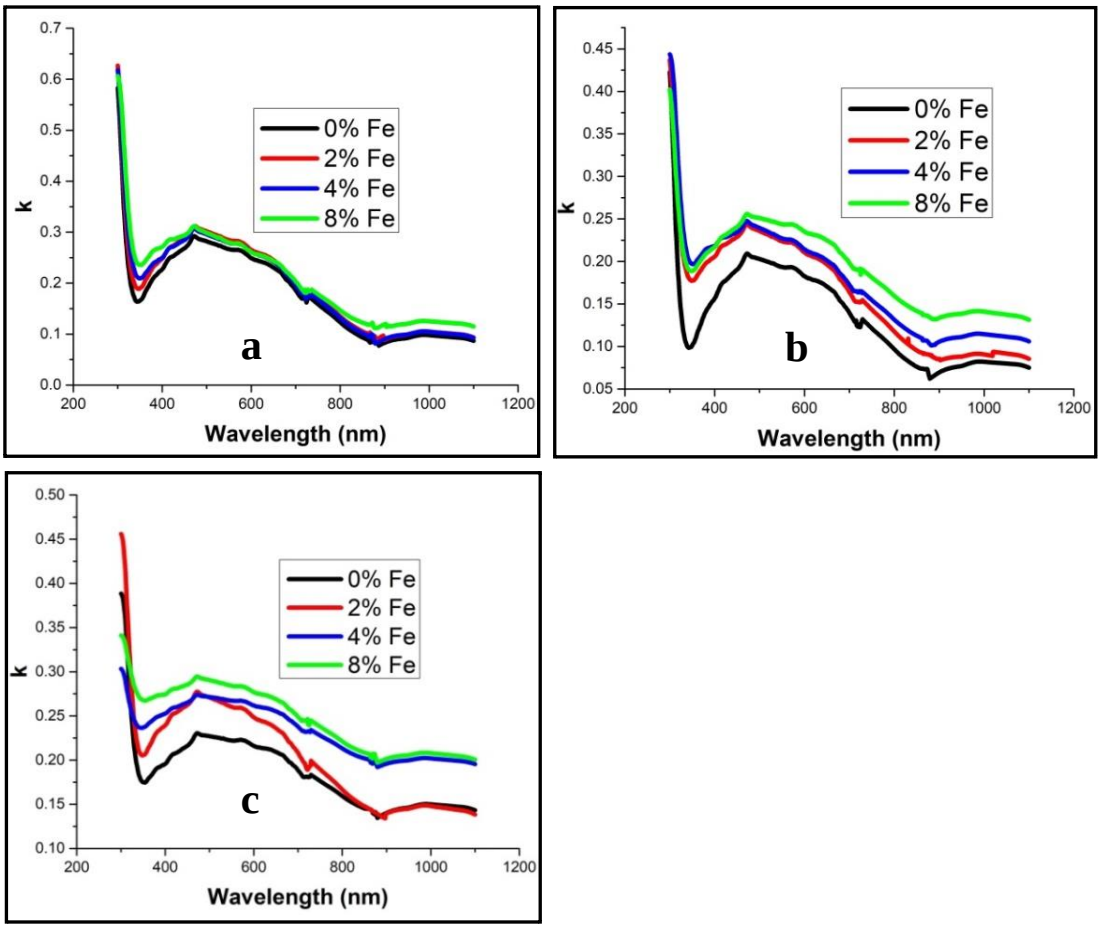

Figure 4.8: Extinction coefficient of (a) 0.1:0.1M Cd_2SnO_4, (b) 0.2:0.2M Cd_2SnO_4 and (c) 0.3:0.3M Cd_2SnO_4 with 0-8% Fe

The increase in extinction coefficient upon doping is due to the increase in the absorption coefficient, which is brought about by the increase in the free charge carriers that absorb more of the incident photons. The values of the extinction coefficient obtained in this study are relatively high, which arise from the relatively lower transmittance obtained.

4.4.4 Refractive index

Refractive indices of the TFs were calculated using equation 2.7. As can be observed in figure 4.9, refractive indices decreased exponentially with an increase in the wavelength, tending to be constant at the long wavelength of above 900 nm. The decrease in refractive index with an increase in the wavelength is due to less reflectance by the TFs at long wavelengths. This agrees with some of the previous work (Dorranian et al, 2012). Xie et al (2012) who studied the optical properties of indium-doped zinc oxide TFs attributed the decrease in refractive index with an increase in the wavelength to an increase in transmission and a decrease in absorption coefficient.

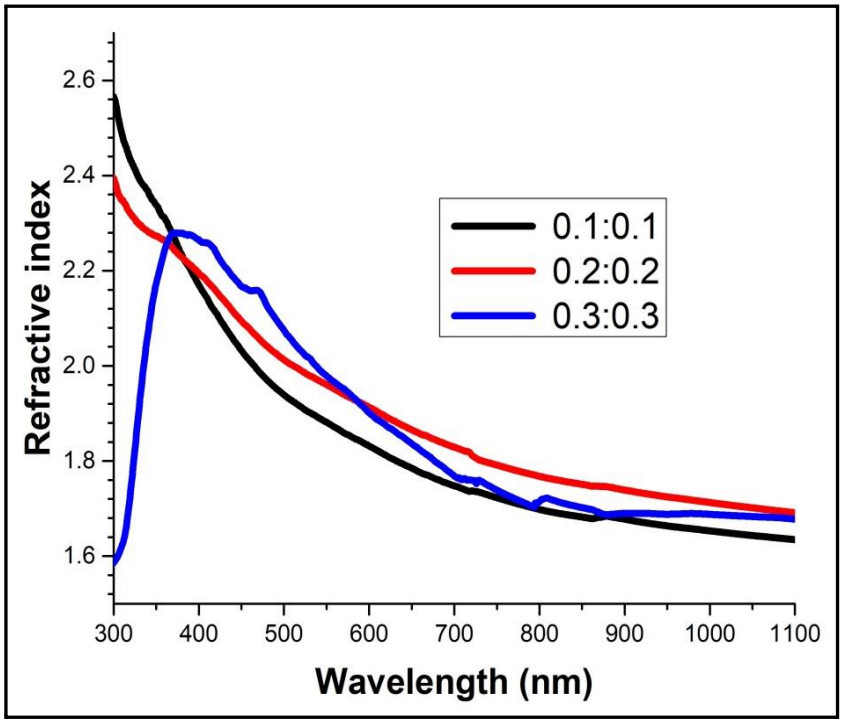

Figure 4.9: Refractive indices of undoped Cd_2SnO_4 TFs at different concentrations

Refractive index was also observed to increase with an increase in the concentration of the reactants. This is due to the increase in reflection by the films. As can be observed in figure 4.9, the concentration of 0.1:0.1M produced TFs with the lowest values of refractive index of 1.844, while those at 0.3:0.3M produced the highest of 1.927 at 588 nm.

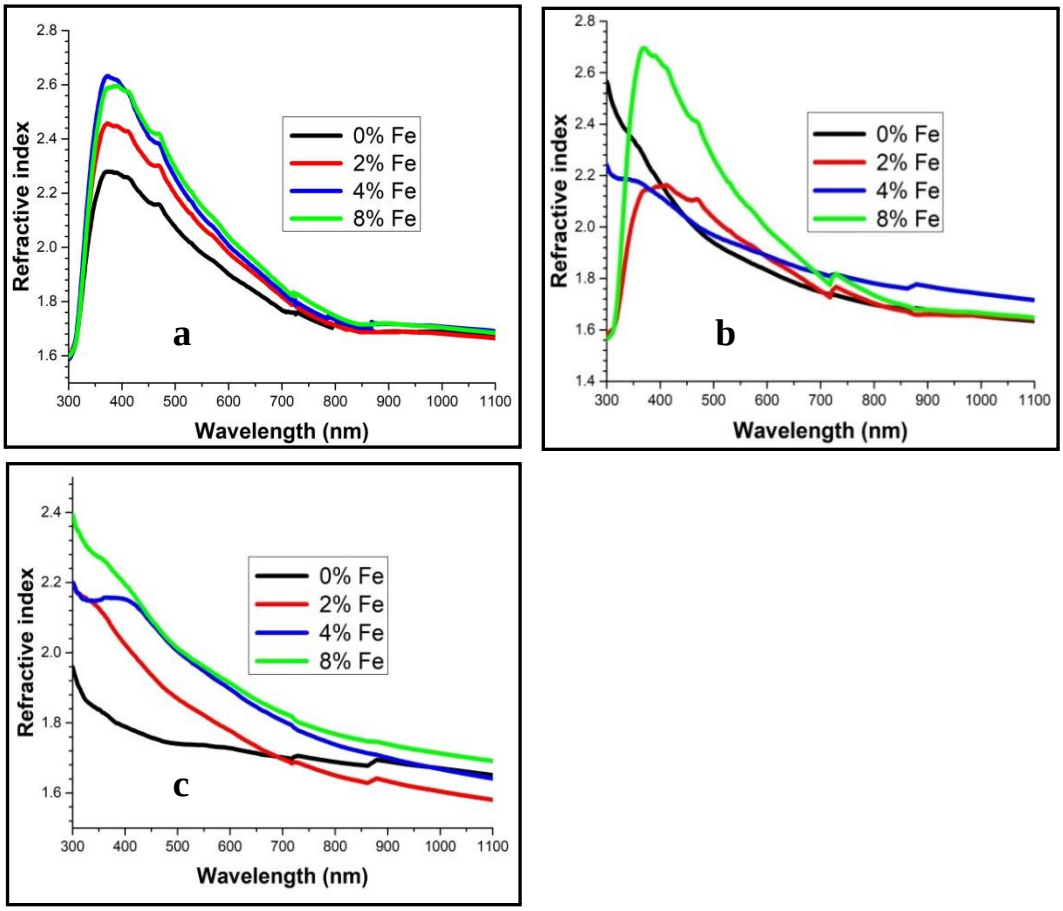

Figure 4.10: Refractive indices of (a) 0.1:0.1M Cd_2SnO_4, (b) 0.2:0.2M Cd_2SnO_4 and (c) 0.3:0.3M Cd_2SnO_4 with 0-8% Fe

The refractive index of 1.844 is close to that of ITO (refractive index of 1.837), the most dominant TCO (Rakesh et al, 2018). The increase in refractive index with an increase in the concentration of the reactants can be explained on the basis that the increase in the concentration of the reactants make the TFs denser (increases the packing density), which in turn decreases the propagation velocity of light through them, since refractive index represents the ratio of light velocity through a vacuum to velocity through a material medium (Bushra and Shallal, 2014).

Doping improved the refractive indices of the deposited TFs as can be observed in figure 4.10, with the concentration of 0.3:0.3M still recording the highest values, while 0.1:0.1M still recording the lowest values. The increase in the refractive indices upon doping is in line with some of the previous work done (Xie, et al, 2012) and is due to the increase in the reflectance, brought about by the free carriers introduced into the TFs by the dopant. The refractive indices of the doped TFs were found to be in the range of 2.00-2.12, which is not good, considering that the increase in refractive index implies an increase in reflectance according to equation 2.7. The increase in reflectance leads to a decrease in transmittance, which not good for TCO materials (Andreas, 2012).

4.4.5 Band gap

The Tauc relation was used to determine the band gap of the deposited TFs. Equation 2.8 was used to calculate the direct band gap. Graphs of $(\alpha E)^2$ were plotted against photon energy (**E = hυ**) in electron volts to obtain figure 4.11.

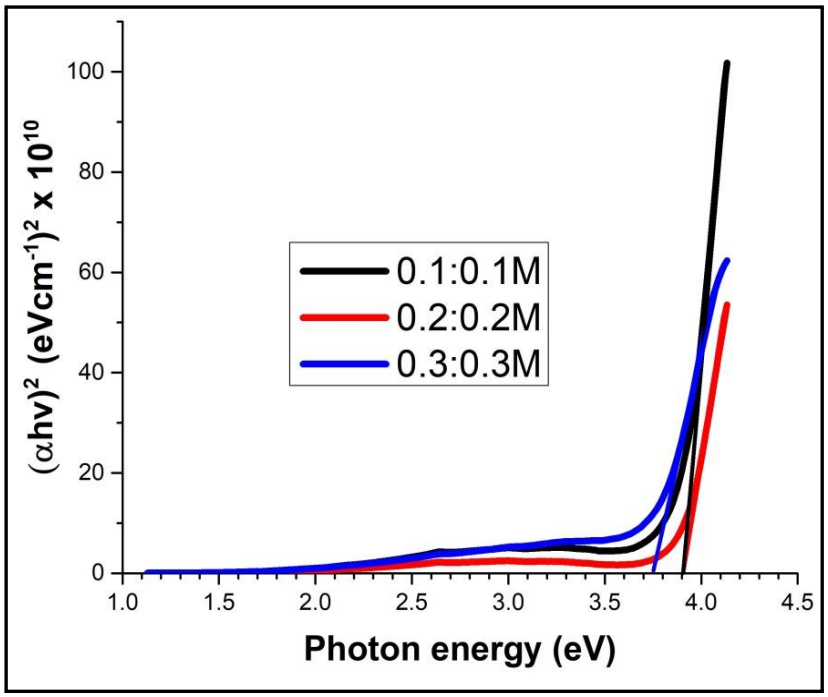

Figure 4.11: $(\alpha hv)^2$ against photon energy for different concentrations of undoped Cd_2SnO_4 TFs

The straight portions of the graphs in figure 4.18 above were extrapolated as shown in figure 4.11. The points where the extrapolated lines intercepted the energy axes (the x-axes) gave the band gap of the deposited TFs in electron volts (Ferro and Rodriguez, 1999).

From the curves obtained in figure 4.11, it was observed that the band gap of the TFs decreased with increase in the concentration of the reactants. This is due to an increase in the reflectance of the films (Hazim, 2014). Ferro and Rodriguez (1999) attributed the decrease in the band gap of cadmium oxide TFs with an increase in the concentration of the reactants to the filling of structural gaps and consequently, filling of the localized states.

The deposited TFs gave a direct allowed transition. The 0.1:0.1M and 0.2:0.2M concentrations gave the highest band gap of 3.9 eV, while the 0.3:0.3M concentration gave the least at 3.75 eV.

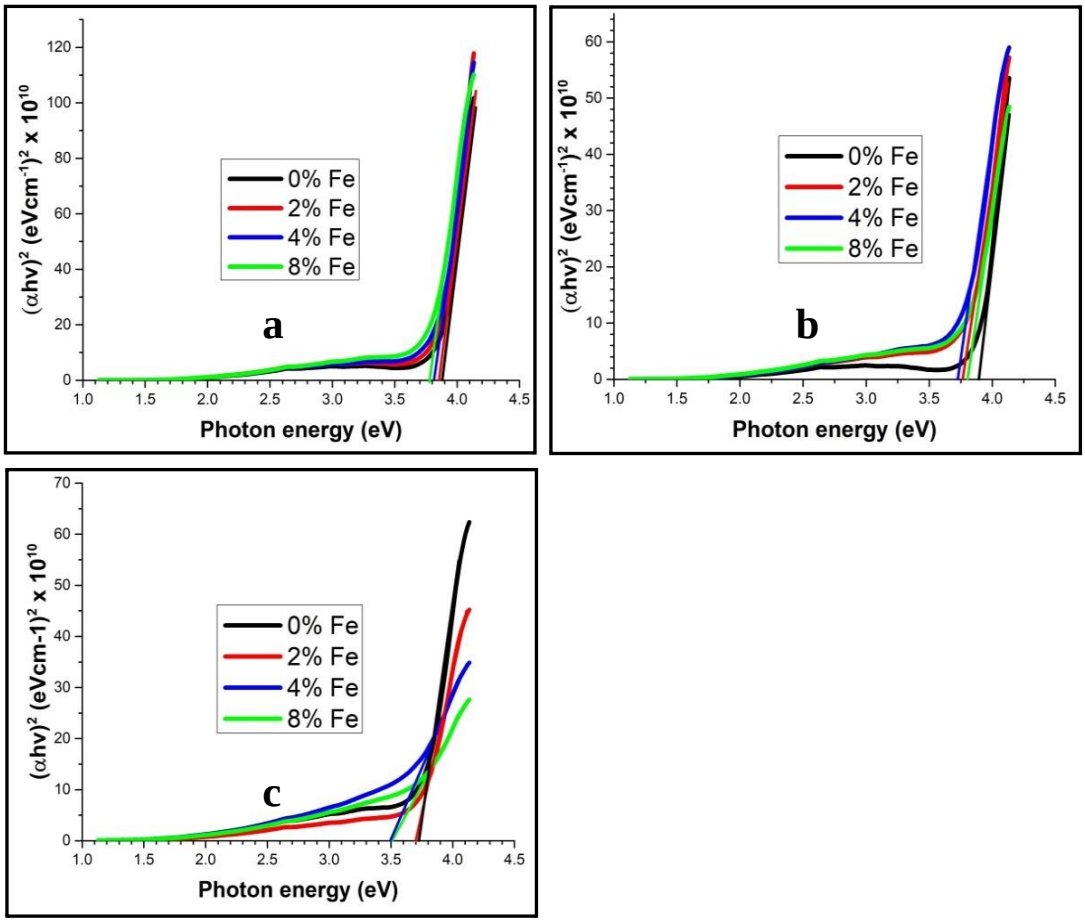

Figure 4.12: (αhv)² against photon energy for (a) 0.1:0.1M Cd_2SnO_4, (b) 0.2:0.2M Cd_2SnO_4 and (c) 0.3:0.3M Cd_2SnO_4 with 0-8% Fe.

Doping lowered the band gaps of the deposited TFs as can be observed in figure 4.12, with the films deposited at a concentration of 0.3:0.3M and doped at 8% recording the lowest values of as low as 3.5 eV (figure 4.12c). The decrease in the band gap with an increase in the concentration of the dopant is due to an increase in the free charge carriers introduced into the TFs by the dopant, which then improve conductivity.

Although a higher band gap is desirable as a property of TCO materials, all the TFs deposited at the different concentrations in figure 4.11 and 4.12 gave band gaps in the range of 3.5-3.9 eV, which are all good for use in TF solar cells, which should have a band gap of greater than 3.2 eV (Minami, 2005). However, a decrease in band gap implies an increase in electrical conductivity, which is a desirable property of TCO materials

The values of the band gap obtained in this study agree well with those found in the literature. Dawar and Joshi (1984) obtained the band gap values of 3.9-4.6 eV.

4.5 Effect of deposition temperature

4.5.1 Transmittance

The 0.1:0.1M TFs were deposited at temperatures of 350 °C, 400 °C and 450 °C. Figure 4.13 shows the results of transmittance obtained.

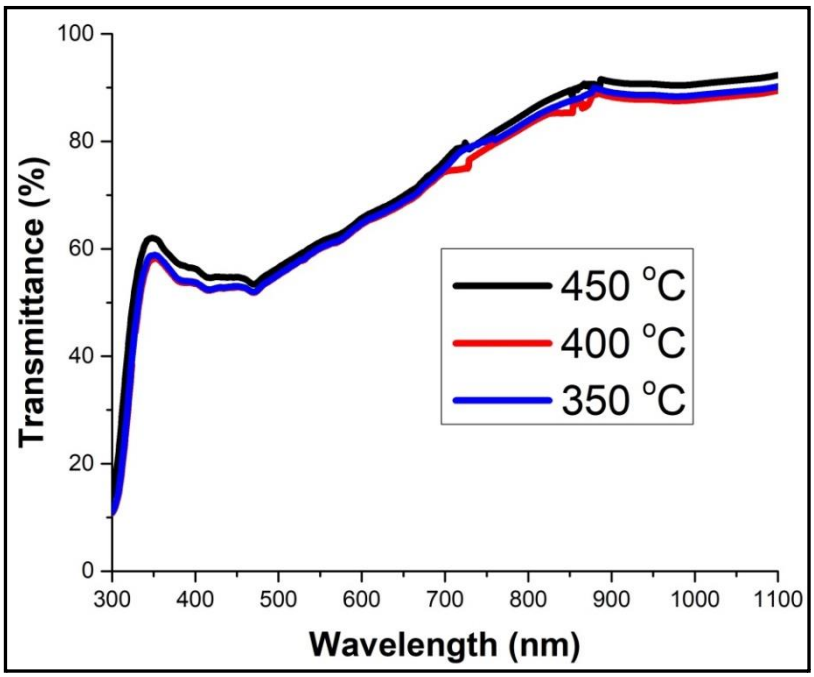

Figure 4.13: Transmittance of undoped 0.1M Cd_2SnO_4 TFs deposited at the three temperatures

The TFs deposited at 450 °C gave the highest transmittance of 78.45%, followed by those deposited at 400 °C at 75.12%. The TFs deposited at 350 °C had the least transmittance of 74.33% at the upper end of the visible spectrum (700 nm wavelength). Jianchao et al (2018) also observed the increase in transmittance with an increase in the deposition temperature in the deposited lanthanum titanate TFs.

The increase in transmittance with an increase in the deposition temperature can be explained by the fact that high deposition temperature enables the Cd_2SnO_4 to land on the substrate in an ordered manner, since high temperature enables the atoms to arrange themselves, thus improving the crystallinity as can be observed in figure 4.2. With the improvement in crystallinity, the light wave scattering decreases, resulting in better transparency of the TFs (Khusayfan and El-Nahass, 2013).

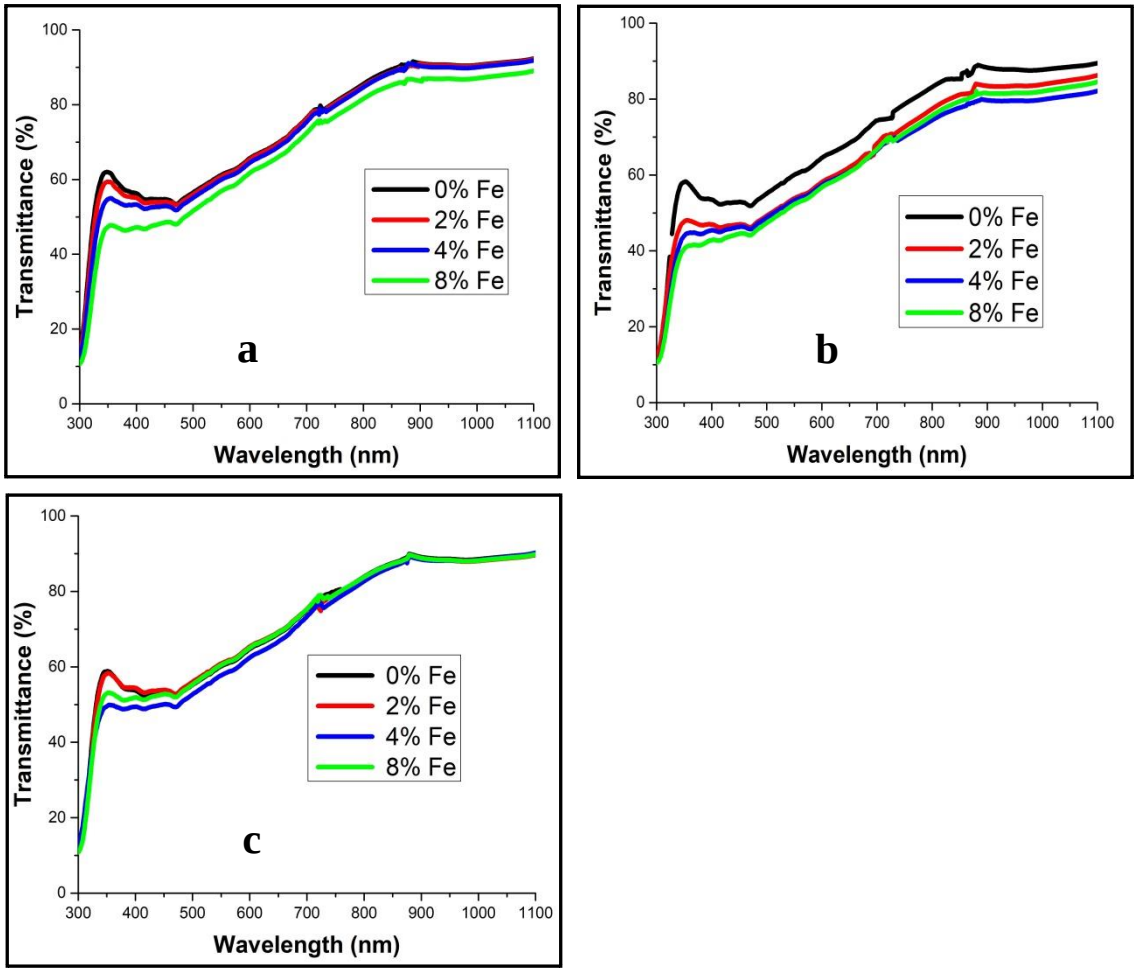

Figure 4.14: Transmittance of 0.1M Cd_2SnO_4 TFs with 0-8% Fe deposited at (a) 450 °C, (b) 400 °C and (c) 350 °C

Long and Cheng (2012) observed that an increase in the deposition temperature results in an increase in the transmittance of the deposited ITO TFs, which they attributed to the increase in the grain size on the surface of the deposited TFs, leading to less scattering of light by decreasing the grain boundaries. The highest transmittance for the TFs deposited at 450 °C in this study also implies that there was low absorbance or reflectance of the incident photons by the TFs at that temperature.

All the curves in figure 4.13 tend to converge at the origin (tend to zero) at short wavelengths below 300 nm. This is due to strong absorption of the incident light by the TFs in the short wavelength range (UV region) (Mulama and Mwabora, 2014).

Figure 4.14 shows the doped TFs at 0-8% Fe at the three deposition temperatures. As can be observed, transmittance decreased with increase in the concentration of the dopant. This is due to the free charge carriers introduced by the dopant, which then absorb and reflect more of the incident photons, thus reducing transmittance. The decrease in transmittance is not a desirable trend for TCO materials.

4.5.2 Absorption coefficient

Figure 4.15 was obtained for the absorption coefficient of the undoped TFs, which shows that the absorption coefficient decreased with an increase in the deposition temperature. The TFs deposited at 350 °C produced the highest absorption coefficient of 5.52188 x 10^4 cm^{-1}, those deposited at 400 °C produced 5.50469 x 10^4 cm^{-1}, while those deposited at 450 °C produced the lowest of 5.29065 x 10^4 cm^{-1}. The decrease in absorption coefficient with an increase in the deposition temperature is due to an increase in free carrier density (Khusayfan and El-Nahass, 2013).

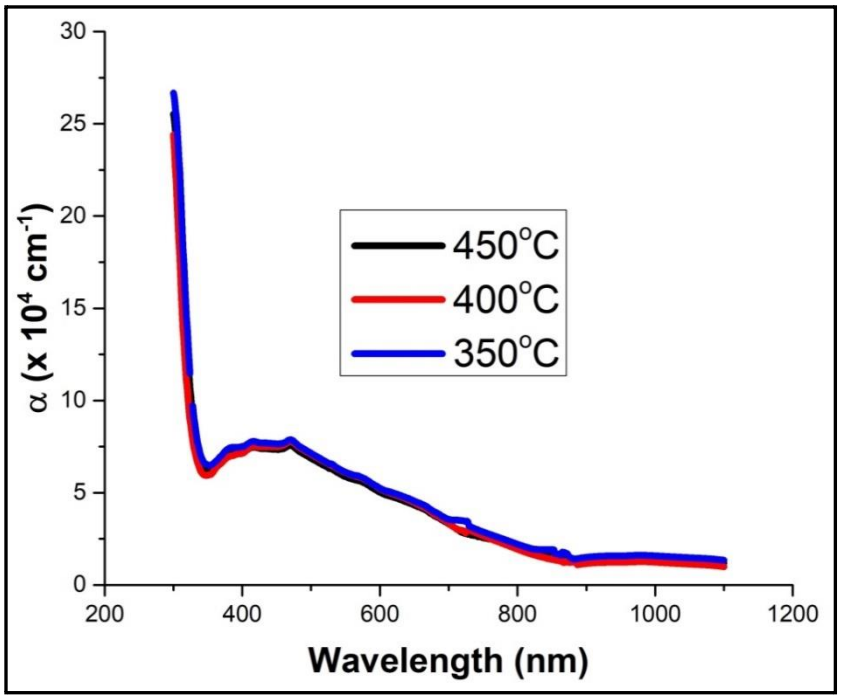

Figure 4.15: Absorption coefficient of undoped 0.1M Cd_2SnO_4 TFs deposited at the three temperatures

All the deposited TFs produced high absorption coefficient of the order of (x 10^4) cm^{-1}. This result is very important because the spectral dependence of the absorption coefficient is one of the important factors which influence the solar conversion efficiency (Khan et al, 2016).

When the TFs were doped, the curves in figure 4.16 were obtained. The absorption coefficient increased with an increase in the concentration of the dopant at all the deposition temperatures, with the 8% Fe giving the highest values. This can be attributed to the increase in carrier absorption with doping. The 8% doped TFs deposited at 350 °C produced the highest absorption coefficient of 5.5381 cm^{-1}.

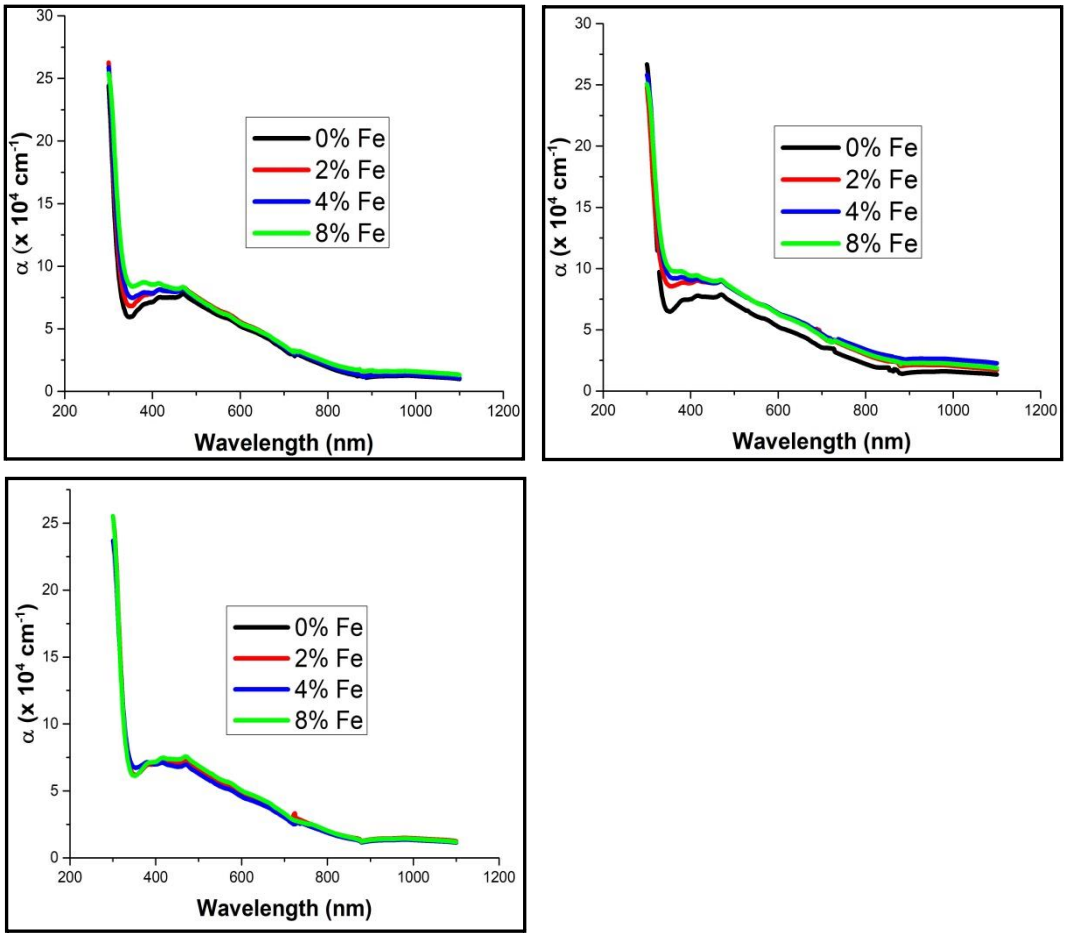

Figure 4.16: Absorption coefficient of 0.1M Cd_2SnO_4 TFs with 0-8% Fe deposited at (a) 450 C, (b) 400 °C and (c) 350 °C

The absorption coefficients obtained in this study are high at short wavelengths, which is good for making front panels of TF solar cells (Ellingson and Heben, 2011).

4.5.3 Extinction coefficient

The graphs of extinction coefficient against photon energy were plotted to obtain figure 4.17.

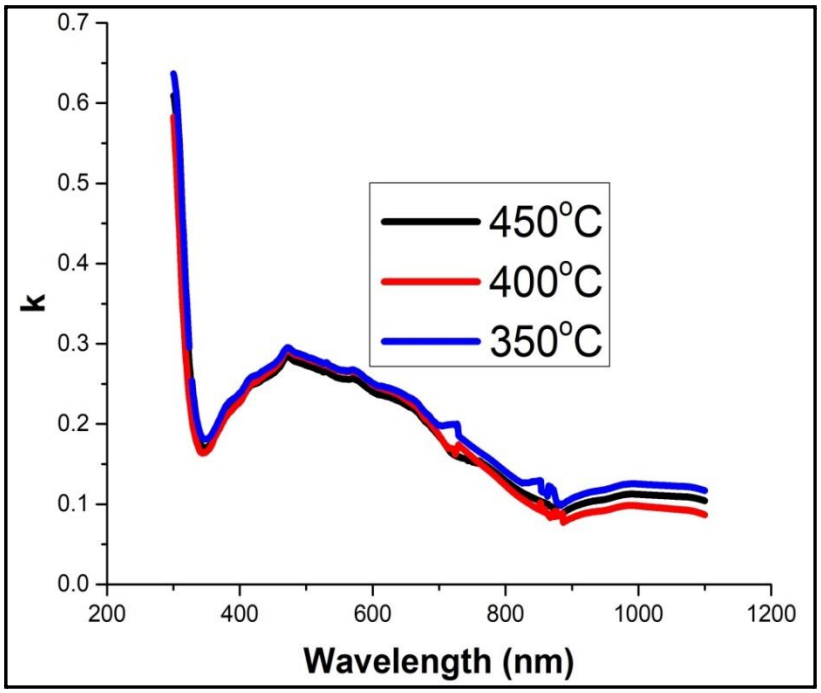

Figure 4.17: Extinction coefficient of undoped 0.1M Cd_2SnO_4 TFs deposited at the three temperatures

Extinction coefficient decreased with an increase in the deposition temperature, same as the absorption coefficient since the two are directly related by equation 2.6. The TFs deposited at 350 °C gave the highest value of extinction coefficient of 0.25834, followed by those deposited at 400 °C with 0.25754. The TFs deposited at 450 °C had the lowest extinction coefficient of 0.24753. Khalifa (2016), who studied titanium IV oxide, also found out that the extinction coefficient of the deposited TFs increased with a decrease in the deposition temperature.

Figure 4.18 shows the curves of the extinction coefficient of the doped TFs. The extinction coefficient increased with an increase in the deposition temperature, which is as a result of an increase in the absorption coefficient. The 8% doped TFs deposited at 350 °C produced the highest extinction coefficient of 0.25832.

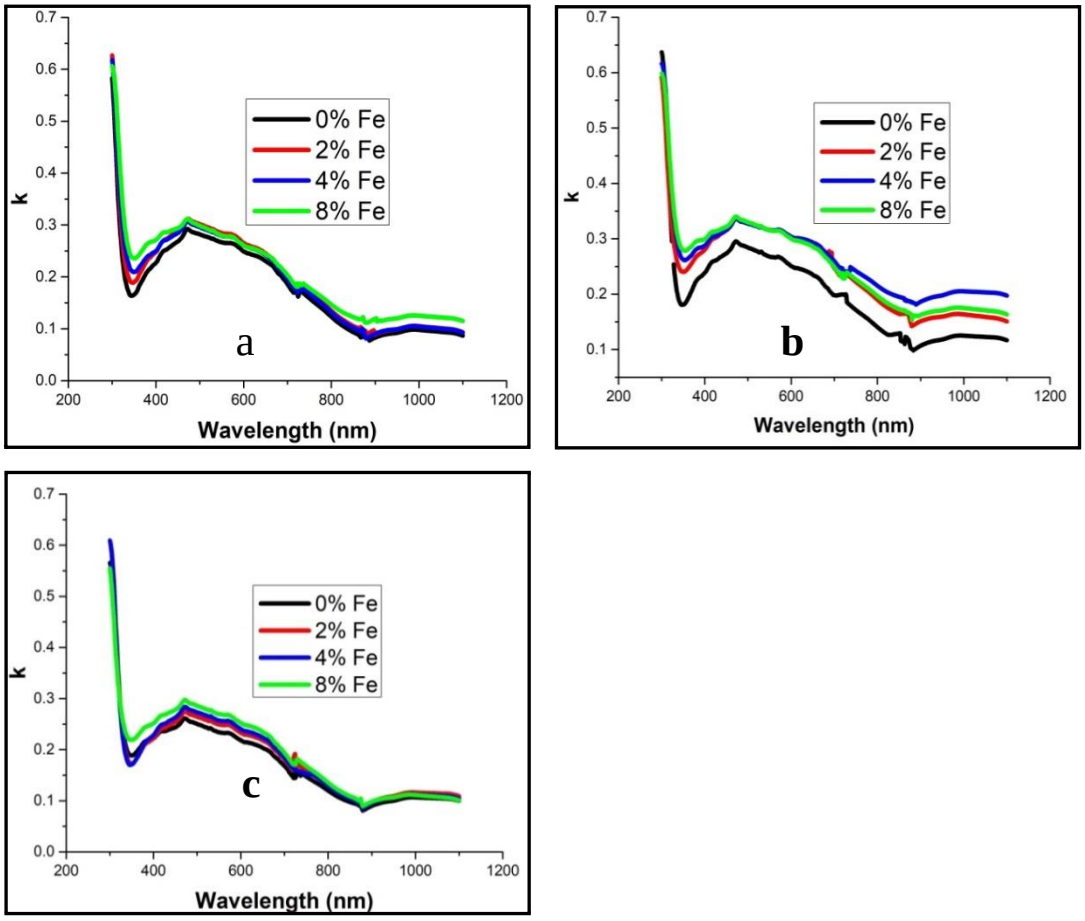

Figure 4.18: Extinction coefficient of 0.1M Cd_2SnO_4 TFs with 0-8% Fe deposited at (a) 450 °C, (b) 400 °C and (c) 350 °C

4.5.4 Refractive index

The graphs of refractive indices of the undoped TFs were plotted against wavelength to obtain figure 4.19.

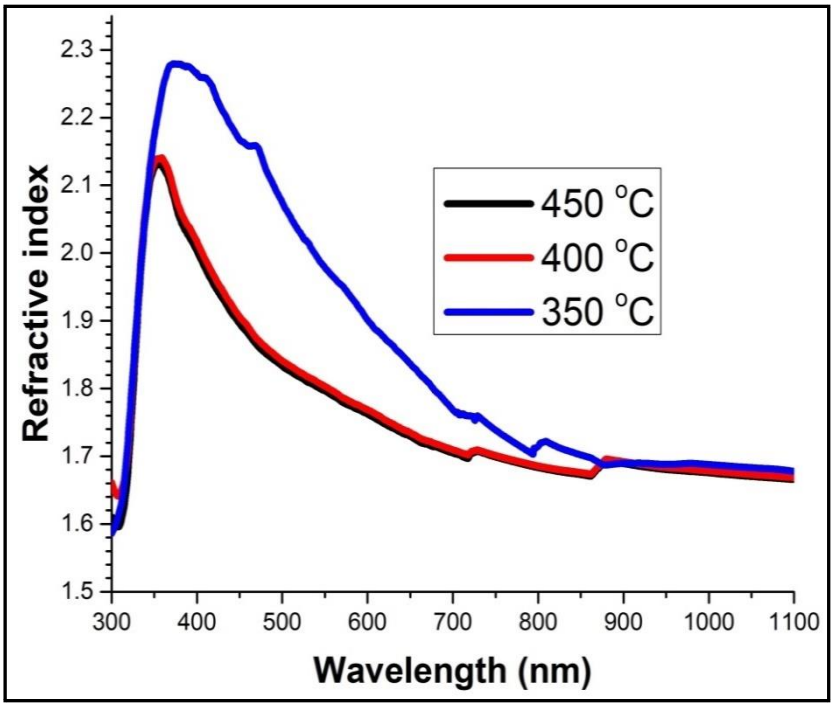

Figure 4.19: Refractive indices of undoped 0.1M Cd_2SnO_4 TFs deposited at the three temperatures

It was observed that the TFs deposited at 450 °C had the lowest values of refractive index, while those deposited at 350 °C had the highest values. This is as was expected, since higher deposition temperatures are supposed to rearrange Cd_2SnO_4 as it lands on the substrate, thus reducing reflectance (Krishna et al, 2010). Refractive indices of all the deposited TFs decreased exponentially with an increase in wavelength, which means low absorption of light at long wavelength range. Khalifa (2016) observed that the refractive index of titanium IV oxide TFs decreased with increase in deposition temperature, which they attributed to the decrease in packing density with an increase in the deposition temperature.

The TFs deposited at 450 °C gave a refractive index of 1.76974, those deposited at 400 °C gave 1.77628 while those at 350 °C gave 1.92305.

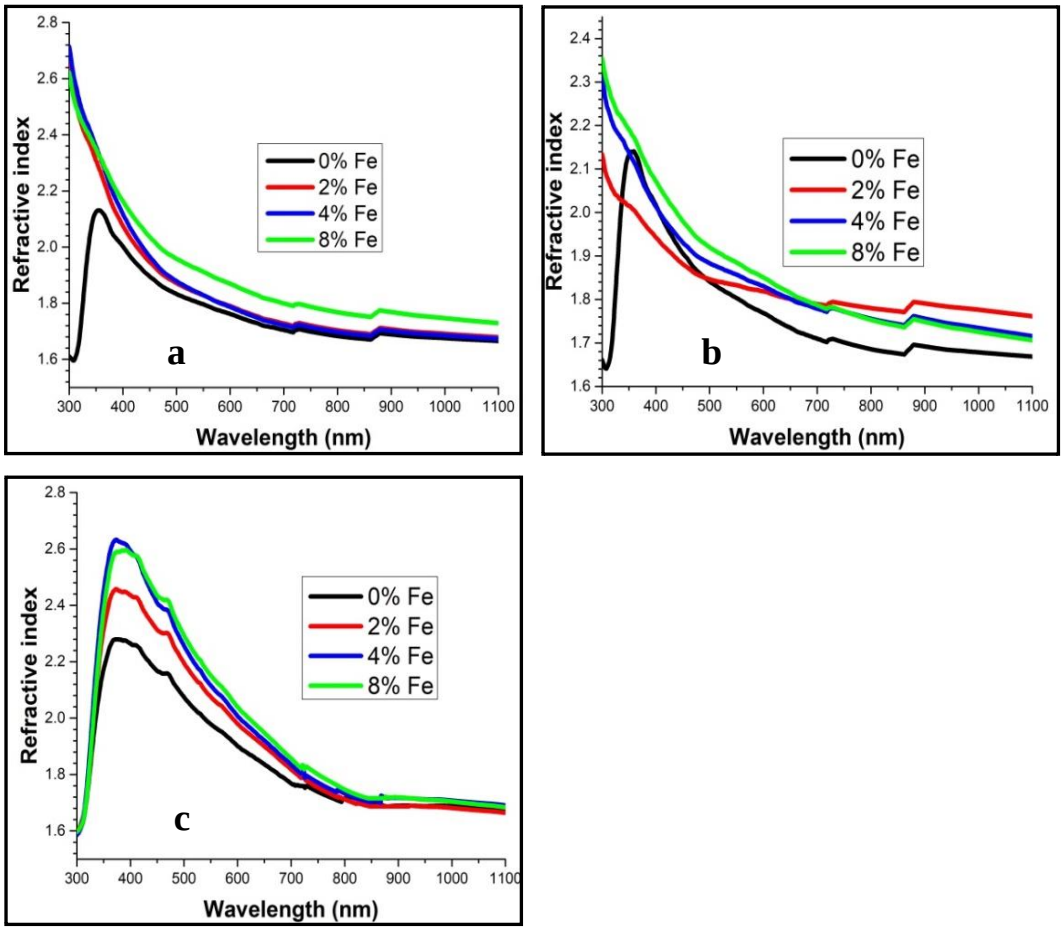

Figure 4.20: Refractive indices of 0.1M Cd_2SnO_4 TFs with 0-8% Fe deposited at (a) 450 °C, (b) 400 °C and (c) 350 °C

The refractive indices still reduced with an increase in deposition temperature upon doping (figure 4.20). The refractive indices were also observed to decrease exponentially with an increase in the wavelength. The doped TFs recorded higher values of refractive indices compared to the undoped TFs, which might have been brought about by the increase in reflectance due to the free carriers introduced by the dopant.

4.5.5 Band gap

The band gap was determined for both the undoped and the doped TFs. The graphs in figure 4.21 show the results obtained.

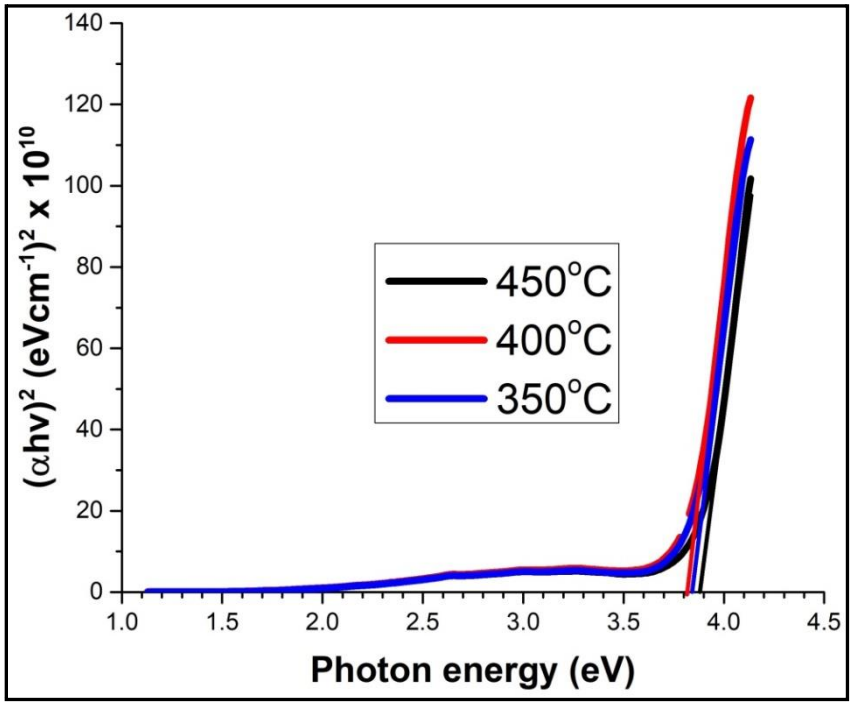

Figure 4.21: $(\alpha hv)^2$ against photon energy for undoped 0.1M Cd_2SnO_4 TFs deposited at the three temperatures

On extrapolating the graphs at the straight portions of the curves to intercept the energy axis, the band gap was found to be 3.9 eV for the TFs deposited at 450 °C, while those deposited at 400 °C and 350 °C both gave a band gap value of 3.8 eV. The highest value of the band gap for the TFs deposited at 450 °C can be attributed to the increase in the crystallinity of the TFs, as can be observed in figure 4.2. Afifi et al (2014) also observed the increase in the band gap of cadmium oxide TFs with an increase in the deposition temperature, which they attributed to change in crystallite size with temperature. Han et al (2012) who researched on indium-zinc-tin-oxide also observed the increase in the bandgap with an increase in the deposition temperature, which they attributed to the effect of Burstein-Mouss shift.

According to Ashok et al (2013), the increase in the band gap with an increase in the deposition temperature is a way of achieving band gap tuning in semiconductor materials and hence, the development of new TFs for efficient photovoltaic application. As the substrate temperature increases, the sharp absorption edge is formed because the grain size increases as TFs become more crystalline.

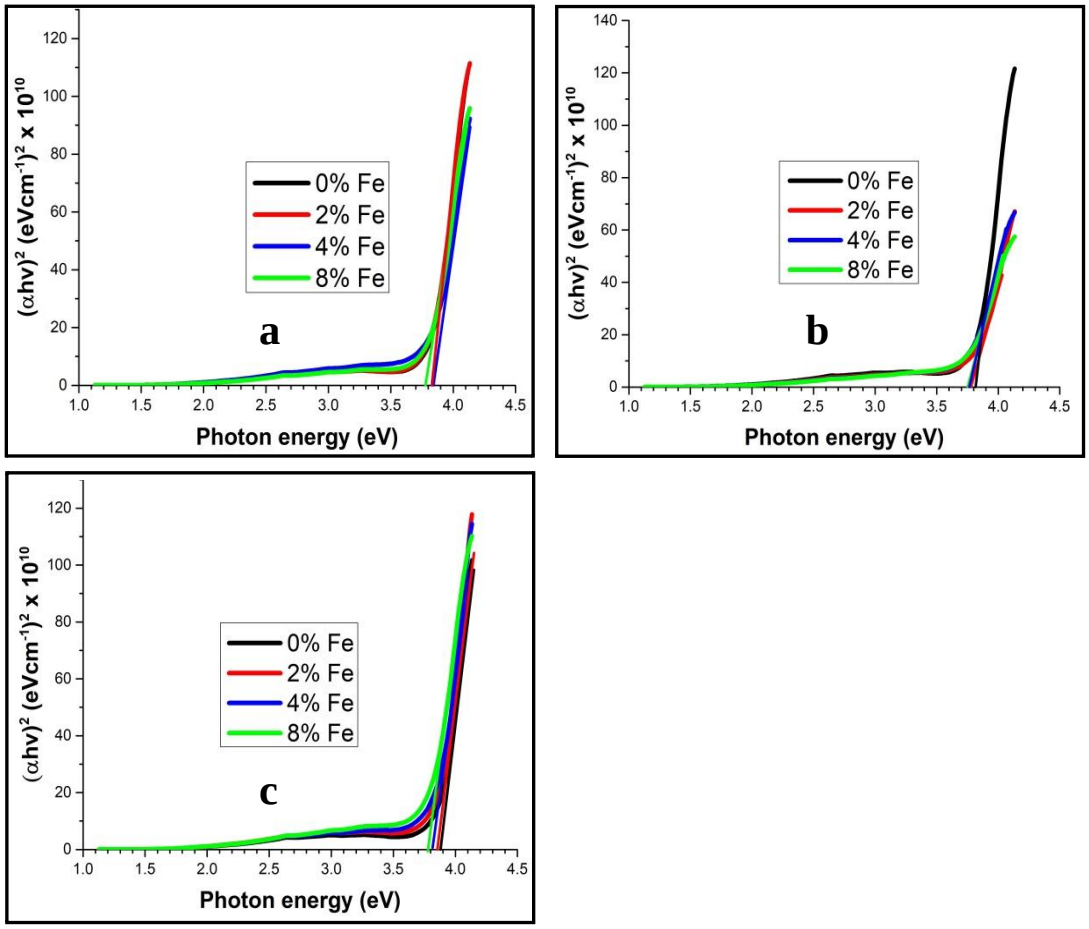

Figure 4.22: $(\alpha hv)^2$ against photon energy for 0.1M Cd_2SnO_4 TFs with 0-8% Fe deposited at (a) 450 °C, (b) 400 °C and (c) 350 °C

When the films were doped, the graphs in figure 4.22 were obtained. The doped TFs registered lower band gaps than the undoped TFs, with the value of the band gap decreasing with an increase in the concentration of the dopant. This is because the absorption edge shifts to higher wavelengths with an increase in the concentration of Fe in the starting solution (Maity and Chattopadhyay, 2005).

4.6 Comparison of the outcome of the present study with some of the published work

The outcome of this research was compared with some of the previous work that have been reported on Cd_2SnO_4. Table 4.3 shows the comparison.

Table 4.3: Comparison of the outcome of the present study with some of the published work

Method	Dopant	T_{max} (%)	k	n_{max}	α (cm^{-1}) x 10^4	Eg (eV)	Refference
SPT	none	99	—	—	—	2.9	Krishna et al, 2010
SPT	none	—	—	2.4	—	2.9-3.3	Alnaimi & Al-Dileamy, 2007
SPT	Chlorine	83	—	—	—	3.1-3.3	Bhuvaneswari & Velusamy, 2013
VET	none	70	.08-.13	2.1	1.9-3.2	2.9-3.1	Eman et al, 2013
SPT	Iron	78	.19-.26	2.06	4.0-5.5	3.75-3.9	Present study

As can be observed in table 4.3, the outcome of the present study agrees very well with those of the previous work done on Cd_2SnO_4. The transmittance, extinction coefficient and refractive index obtained in the present study fall in between those of the previous studies. However, the absorption coefficient and band gap appear to be a little bit higher than some of the previous studies that have been obtained.

CHAPTER FIVE
CONCLUSION AND RECOMMENDATIONS

5.1 Conclusion

5.1.1 Effect of concentration of reactants

The optical properties were observed to vary with the concentration of cadmium acetate and tin II chloride.

i. The concentration of 0.1M Cd_2SnO_4 produced TFs with the highest transmittance of 78.45% at the upper end of the visible spectrum (700 nm), while the concentration of 0.3M gave the lowest transmittance of 64.27%. Doping reduced the transmittance of the TFs, with the heavily doped TFs recording the lowest values.

ii. Absorption coefficient increased with increase in the concentration of the reactants. The concentration of 0.1:0.1M gave the lowest value of 4.022×10^4 cm^{-1}, while the 0.3:0.3M concentration gave the highest of 5.505×10^4 cm^{-1} at the upper end of the visible spectrum of 700 nm. Upon doping, the absorption coefficient increased.

iii. The extinction coefficient of the deposited TFs increased with increase in the concentration of the reactants. The 0.1:0.1M concentration gave 0.188, while the 0.3:0.3M gave 0.254. Upon doping, the values increased.

iv. Refractive index was observed to increase with an increase in the concentration of the reactants, with values in the range of 1.844-1.925. Doping improved the refractive index of the deposited TFs, with the 8% Fe giving the highest values to a maximum of 2.069.

v. The band gap decreased with increase in the concentration of the reactants. A band gap of 3.9 eV was obtained for the TFs deposited at the concentration of 0.1:0.1M and 0.2:0.2M, while the concentration of 0.3:0.3M gave a band gap of 3.75 eV. Upon doping, the band gaps reduced with an increase in the concentration of the dopant.

5.1.2 Effect of deposition temperature

i. The TFs deposited at 450 °C recorded the highest transmittance of 78.45% at the upper end of the visible spectrum, while those deposited at 350 °C recorded the least at 74.77%. The TFs deposited at 400 °C recorded a transmittance of 78.04%. Doping the TFs reduced the transmittance at all the three temperatures, with the value of transmittance decreasing with increase in the concentration of the dopant.

ii. Absorption coefficient reduced with an increase in the deposition temperature. The TFs deposited at 450 °C recorded the lowest value of $5.291 \times 10^4\ cm^{-1}$, while those deposited at 350 °C recorded a value of $5.505\ cm^{-1}$ at the upper end of the visible spectrum. Doping improved the absorption coefficient.

iii. Extinction coefficient reduced with an increase in the deposition temperature. The TFs deposited at 350 °C recorded the highest value of extinction coefficient of 0.258, while those deposited at 450 °C recorded the least value of 0.248. Doping increased the extinction coefficient.

iv. Refractive index decreased with an increase in the deposition temperature. Those deposited at 450 °C gave the lowest value of 1.770, while those deposited at 350 °C gave the highest value of 1.923. Doping increased the refractive indices at all the three deposition temperatures.

v. The band gap decreased with increase in the deposition temperature, with a value of 3.9 eV for those deposited at 450 °C, while those deposited at 400 °C and 350 °C both gave a value of 3.85 eV. Doping reduced the band gap at all the three deposition temperatures, with the band gap value reducing with an increase in the concentration of the dopants.

5.2 Recommendations

5.2.1 Applications

1) In the front panels of TF solar cells, which require absorption coefficient of $\geq 10^4$ cm^{-1}, transmittance of ~80% and above (Andreas, 2012), reflectance of less than 10% and a band gap of above 3.2 eV (Siefert, 1984). The TFs deposited at a concentration of 0.1:0.1M and at a temperature of 450 °C gave a transmittance of 78.45% in the visible spectrum, an absorption coefficient of 5.522 x 10^4 cm^{-1} and a band gap of 3.9 eV, making the TFs to be photosensitive in the visible spectrum. The TFs can be used in making TF solar cells, which will improve the lives of the common Kenyan citizens.
2) Addition of the dopant lowers the band gap of the deposited Cd_2SnO_4 from 3.9 eV to 3.5 eV, which leads to an improvement in the electrical conductivity. The TFs can therefore be applied in the smartphone touch screens (Kolokowsky and Davis, 2009).
3) Window films, since the TFs have high transmittance in the (NIR) wavelength range of up to 97%. Thus, they can be used in making window panes that will allow heat into the rooms during winter. They can also be used in xerographic systems which receive radiation that is out of the visible spectral wavelength range. The TFs of Cd_2SnO_4 can also be employed as the photoconductor layer for use in the flat panel x-ray image detector and high definition video camera.
4) Infrared touchscreens, which require high transmittance in the infrared spectral wavelength region. The touch screens are used in outdoor applications and point of sale systems.

5.2.2 Further studies

1) Optical properties alone are not enough for good use in the areas mentioned above. In order for the TFs to be of good use, other properties like electrical and mechanical need to be factored in. Therefore, research on those properties needs to be carried out.
2) Doping of the Cd_2SnO_4 with other metals such as zinc and tellurium can also be carried out to determine their effect on the optical properties the TFs.
3) The surface morphology of the TFs also needs to be studied so as to investigate its effect on the optical properties Cd_2SnO_4.
4) The study concentrated on the optical properties of Cd_2SnO_4 without further treatment. There is, therefore, need to investigate the effect of annealing of the TFs both in vacuum and in air on their optical properties.
5) Deposition of the TFs was done only at the symmetric concentrations (0.1:0.1M, 0.2:0.2M and 0.3:0.3M). The non-symmetric concentrations (0.1:0.2M, 0.1:0.3M, 0.2:0.1M e.t.c) also need to be studied in order to investigate their effect on the optical properties of the TFs.

REFERENCES

1. Afifi, H. H. Ahmed, N. M. Tadros, M. T. Y. Ibrahim, F. M. (2014). Temperature dependence growth of CdO thin film prepared by spray pyrolysis, *Journal of Electronic System and Information Technology*, http://dx.doi.org/10.1016/j.jesit.2014.07.001
2. Alnaimi, S. M. & Al-Dileamy, M. N. (2007). *Determination of optical constants of cadmium stannate films.* Doha: University of Qatar.
3. Andreas, S. (2012). Transparent conducting oxides: An up-to-date overview. *Materials*, **2012** (5), 661-683.
4. Ashok, CH. Venkateswara, R. K. Shilpa, C. & Ganapathi, R. K. (2013). Structural and optical properties of CdS thin films for solar cell applications. *International Journal of Science and Research (IJSR),* **1** (1), 2319-7064.
5. Ayre, J. (2014). New CIGS solar cell record-21.7% CIGS cell conversion efficiency achieved at ZSW. *Clean Technica*, **3** (9), 39-48.
6. Baker, S. (2012). TFT central. *Panel Coating*, **2** (8), 3-11.
7. Bhuvaneswari, P. & Velusamy, M. A. (2013). Effect of fluorine doping on the structural, optical and electrical properties of spray deposited cadmium stannate thin films. *Materials Science in Semiconductor Processing*, **16** (2013), 1964-1970.
8. Bright, C. (2013). Transparent conductive thin films. *Optical Thin Films and Coatings,* **1**(1), 741-748.
9. Bushra, A. H. & Shallal, I. H. (2013). Structural and optical properties of SnS thin films. *Journal of Nanotechnology and Advanced Materials*, **2** (2), 43-49.
10. Butcher, J. B. & Pitt, K. E. G. (2009). Thick films in electronics. *Electronics and Power*, **8** (17), 17-20.
11. Calleja, A. Susagna, R. Aklaluoch, M. & Mestres, N. (2014). Thickness-concentration-viscosity relationships in spin-coated metalorganic ceria films containing polyvinylpyrrolidone, *Journal of Sol-Gel Science and Technology* **1** (1), 1-24.
12. Chopra, K. L. Major, S. & Pandya, D. K. (1983). Transparent conductors-A status review. *Thin Solid Films*, **102** (1983), 1-46.
13. Clark, A. (1980). *Polycrystalline and amorphous thin films and devices.* New York: Wiley and Sons Inc.

14. Cole, J. (2013, May 16). Kenya gets funding for Africa's largest wind firm. Retrieved from https://www.juancole.com
15. Coutts, T. J. Yong, D. L. & Xiaonan, L. (2000). Characterization of transparent conducting oxides. *MRS BULLETIN/ August 2000*. 58-65
16. Cristaldi, A. Gulino, A. & Maria, E. F. (2012). Structural, electronic and electrical properties of yttrium-doped cadmium stannate. *Journal of Physical Chemistry*, **116** (5), 3363-3368.
17. Cullity, B. D. & Stock, S.R. (2001). *X-ray diffraction*. London: Prentice Hall.
18. Dawar, A. L. & Joshi, J. C. (1984). Semiconducting transparent thin films: their properties and applications. *Journal of Material Science*, **19** (1984), 1-23.
19. DeBusk, S. (2015). Comparative analysis of retrofit window film to replacement with high-performance windows. *CP Films*, **7** (4), 1-8.
20. Definitive solar (2018, April 13). Retrieved from http://www.definitivesolar.com
21. Dislich, H. & Hinz, P. (October 1980). Process for producing cadmium stannate layers. Retrieved from http://www.freepatentsonline.com/4229491.html. Accessed: 18/03/2010.
22. Du, J. Chen, X. Liu, C. Ni, J. Hou, G. Zhao, Y. & Zhang, X. (2014). Highly transparent and conductive indium tin oxide thin films for solar cells grown by reactive thermal evaporation at low temperature. *Applied Physics A*, **117** (2), 815-822.
23. Ellingson, R. & Heben, M. (2011). *Absorption coefficients of semiconductor thin films.* Toledo: University of Toledo.
24. Eman, N. Igbal, S. N. & Alias, M. F. (2013). Characterization of cadmium tin oxide thin films as a window layer for solar cell. *International Journal of Application and Innovation in Engineering and Management*, **2** (9), 189-194.
25. Eman, N. (2014). *Optical and electrical properties of cadmium tin oxide films prepared by vacuum evaporation technique.* Baghdad: University of Baghdad.
26. Ferro, R. & Rodriguez, J. A. (1999). Some physical properties of F-doped CdO thin films deposited by spray pyrolysis. *Thin Solid Films*, **347** (1999), 295-298
27. Gauckler, L. J. (2005). Thin film deposition using spray pyrolysis. *Journal of Electroceramics*, **14** (1), 103-111.
28. Golestani-Fard, F. & Mackenzie, K. JD. (1983). Formation of cadmium stannate studied by electron spectroscopy. *Journal of Materials Science*, **18** (1983) 3679-3685.

29. Green, M. A. (2007). Thin film solar cells: Review of technologies and commercials status. *Journal of Materials Science: Materials in Electronics*, **18** (1), 1-10.
30. Green, M. A. (2003). Crystalline and thin-film silicon solar cells: State of the art and future potential. *Solar Energy*, **74** (3), 181-192.
31. Grolik, B. & Kopp, J. (2003). *Optical properties of thin semiconductor films.* Sydney: Wiley and Sons Inc.
32. Hazim, L. M. (2014). Structural and optical properties of CdSe thin films prepared by CBD. *International Journal of Thin Films Science and Technology*, **3** (2), 57-60.
33. Hummel, R. E. (2001). *Electronic properties of materials, 3rd Edition.* New York: Springer.
34. Jeyadheepan, K. & Sanjeeviraja, C. (2014). Preparation and crystal structures of some $A^{IV}B_2^{II}O_4$ compounds: Powder X-ray diffraction and Rietveld analysis. *Journal of Chemistry*, 2014 (1), 1-6.
35. Jianchao, L. Wanmin, Y. Junhong, S. & Chen, Y. (2018). Effects of deposition temperature on structural, optical properties and laser damage of $LaTiO_3$ thin films. *Advances in Condensed Matter Physics*, **2018** (1), 1-6.
36. Khalifa, Z. S. (2016). Effect of deposition temperature on the properties of TiO_2 thin films deposited by MOCVD. *Surface Review and Letters*, **23** (2), 1-9.
37. Khan, M. A. Ahmed, A. Ali, N. Igbal, T. Maboob, U. & Shafique, M. (2016). Improved optical properties of tin-antimony sulphide thin films for photovoltaics. *American Journal of Materials Science and Engineering*, **4** (1), 1-6.
38. Khusayfan, N. M & El-Nahass, M. M. (2013). Study of structure and electro-optical characteristics of indium tin oxide thin films. *Advances in Condensed Matter Physics*, **2013** (1), 1-8.
39. Kolokowsky, S. & Davis, T. (2009). Touchscreens 101: Understanding touchscreen technology and design. *Cypress Semiconductor Corporation*, **1** (1), 1-5.
40. Krishna, K. Kamamurthi, K. & Elangovan, E. (2009). *Novel procedure to prepare cadmium stannate films using spray pyrolysis technique for solar cell applications*. *Current Applied Phys*ics **9** (2009) 467-471.
41. Kuo, L. (2017). Kenya's national electrification campaign is taking less than half the time it took America. New York: Quartz Africa.

42. Long, B. & Cheng, S. (2012). Properties of indium tin oxide films deposited by RF magnetron sputtering at various substrate temperatures. *Micro and Nano Letters*, **7** (8), 835-837.
43. Maity, R. & Chattopadhyay, K. K. (2006). Synthesis and characterization of aluminium-doped CdO thin films by sol-gel process. *Solar Energy Materials & Solar Cells*, **90** (2006), 597-606.
44. Makori, N. E. Amatalo, I. A. Karimi, P. M. & Njoroge, W. K. Optical and electrical properties of CdO: Sn thin films for solar cell applications. *International Journal of Optoelectronic Engineering*, **4** (1), 11-15.
45. Marozau, I. S. (2009). Optical properties of nitrogen-substituted strontium titanate thin films prepared by pulsed laser deposition. *Materials*, **2** (1), 1388-1401.
46. Mazzeo, M. Mariano, F. & Gigli, G. (2013). High-efficiency ITO-free flexible white organic light-emitting diodes based on multi-cavity technology. *Organic Electronics*, **4** (12), 2840-2846.
47. Meyers, H. P. (1990). *Introductory solid state physics*. London: Taylor & Francis.
48. Meysing, D. M. Burst, J. M. Rance, W. I. Reese, M. O. Barnes, T. M. Gessert, T. A. & Wolden, C. A. (2013). The influence of cadmium sulphide and contact annealing configuration on the properties of high-performance cadmium stannate. *Solar energy materials and solar cells*. 117 (2013), 300-305.
49. Minami, T. (2005). Transparent conducting oxide semiconductors for transparent electrodes. *Semiconductor Science and Technology*, **20** (4), 35-44.
50. Mohammad, M. T. & Ghafor, W. A. A. (1989). Optical properties of cadmium stannate thin film prepared by pyrolytic process. *Solid State Communications*, **72** (1), 1043-1046.
51. Mott, N. F & Davis, E. A. (1979). *Electric processes in non-crystalline materials. 2nd Edition.* Oxford: Clarendon Press.
52. Mulama, A. & Mwabora, J. M. (2014). Optical properties and raman studies of amorphous Se-Bi thin films. *The African Review of Physics*, **9** (6), 32-38.
53. Mulama, A. Mwabora, J. M. & Oduor, A. O. (2014). Investigation of the effect of film thickness on the optical properties of amorphous $Se_{85-x}Te_{15}Sb_x$ thin films. *Africa Journal of Physical Sciences*, **1** (1), 37-42.

54. Ohring, M. (1992). *The material science of thin films.* London: Academic Press.
55. Patil, L. A. Dea, V. V. & Kaushik, M. P. (2012). Modified cadmium stannate nanostructured thin films prepared by spraying technique for detection of chemical warfares. *Pratibha: International Journal of Science, Spirituality, Business and Technology*, **1** (1), 2261-2277.
56. Pearce, J. & Lau, A. (2002). Net energy analysis for sustainable energy production from silicon-based solar cells. *International Solar Energy Conference* (pp. 181-186). Nevada: Solar Energy.
57. Rakesh, A. A. Nallin, S. M. & Madhuri, S. (2018). Transparent conducting oxide films for various applications: A review. *Review of Advanced Material Science*, **53** (2018), 79-89.
58. Rauschenbach, H. S. (1980). *Solar cell array design.* New York: Van Nostrand Reinhold Co.
59. Sakthivel, P. Murugan, R. Asaithambi, S. & Ravi, G. (2018). Studie on optoelectronic properties of magnetron sputtered cadmium stannate (Cd_2SnO_4) thin films as alternative TCO materials for solar cell applications. *Ceramics International*, **44** (2018), 2529-2538
60. Samar, Y. Dabagh, Al. & Eman, E. M. (2016). The effect of Fe concentration on the structure and optical properties of ZnO films by using pulsed laser deposition. *IOSR Journal of Dental and Medical Sciences (IOSR-JDMS)*, **15** (20), 54-60.
61. Setty, M. S. & Sinha, A. P. B. (1986). Characterization of highly conducting Pb-doped Cd_2SnO_4 thick films. *Thin Solid Films*, **144** (1986), 7-19.
62. Shugar, G. & Ballinger, J. (1996). *Chemical technicians' ready reference handbook.* New York: McGraw-Hill.
63. Siefert, W. (1984). Thin solid films. *Journal of Electronics*, **120** (4), 265-271.
64. Tam O. S. & Stockton, Dr. (2012). Energy analysis for window films applications in new and existing homes and offices. *International Window Film Association*, **1** (1), 1-23.
65. Warren, B. E. (1990). *X-ray diffraction*. New York: Dover Publications Inc.
66. Wu, X. Sheldon, P. Coutts, T. J. Rose, D. H. & Moutinho, H. R. (1997). *Application of Cd_2SnO_4 transparent conducting oxides in CdS/CdTe thin-film device*s. Anaheim: National Renewable Energy Laboratory (NREL).

67. Xie, C. G. Fang, L. Peng, L. P. Liu, G. B. Ruan, H. B. Wu, F. % Kong, C. Y. (2012). Effect of In-doping on the optical constants of ZnO thin films. *Physics Procedia*, **32** (2012), 651-657.
68. Yang, M. Su, X. & Tang, A. Mechanochemical synthesis of cadmium-doped tin oxide nanoparticles. *International Journal of Nanoscience,* **5** (1), 91-98.